



UNIVERSITY *of the*
WESTERN CAPE

**POLYDOPAMINE COATED PLATINUM
CATALYSTS TO IMPROVE
FUEL CELLS DURABILITY**

By

Ange Mireille Mugeni (3459241)

Being

A Thesis submitted in fulfilment of the requirement for the award of the degree of
Master of Science in the Department of Chemistry, University of The Western Cape

January 2022

Supervisor: Prof. Lindiwe Khotseng

Co-supervisor: Dr. Jessica Chamier

<http://etd.uwc.ac.za/>

KEYWORDS

- ❖ Proton exchange membrane fuel cells
- ❖ Catalysts
- ❖ Oxygen reduction reaction
- ❖ Electrochemistry
- ❖ Electrocatalyst
- ❖ Carbon support
- ❖ Corrosion Resistance
- ❖ Electrolyte
- ❖ Oxidation
- ❖ Reduction



DECLARATION

I hereby declare that, “**Polydopamine coated Platinum catalysts to improve Fuel Cells durability**” is my own work and it has not been submitted before for any degree or examination in any other university, and all the sources I have used or quoted have been indicated or acknowledged by way of complete references.

Ange Mireille Mugeni

Signed:



12 January 2022

ABSTRACT

Polymer electrolyte membrane fuel cells (PEMFC) are in the forefront of energy production and have drawn a great deal of attention in both fundamental and application in recent years. It is a promising energy system used in commercialized electric vehicles presenting with the following advantages: low-temperature operation, high power density (40%–60%), nearly zero pollutants compared to conventional internal combustion gasoline vehicles, simple structure, and so on. There are, however, two major obstacles which obstruct PEMFCs pathway to commercialization—durability and cost. Recent advances in PEMFC systems showed the most common fuel cell catalysts to be Platinum (Pt) (or platinum alloys) supported by high surface carbon in both the cathode and anode. However, carbon is very susceptible to corrosion and results in lower durability of Pt supported catalysts.

The rate of the oxygen reduction reaction (ORR) occurring in the cathode catalyst layer primarily determines the cell voltage, as the rate of the anodic reaction is considerably faster by comparison. The characteristics of the cathode catalyst layer, therefore, have a huge impact on the overall performance of PEMFC. Successful commercialization requires ORR electrocatalysts that can meet performance targets, are low in cost and are highly durable. Currently not all proposed approaches meet these demands. This study was performed to improve the durability of the Pt catalyst by means of material modification without compromising the ORR performance of the catalyst. This encompasses a mitigation strategy in which the surface of the carbon support is chemical modified to reduce the effect of carbon degradation.

Recent studies of Polydopamine (PDA), the final oxidation product of dopamine or other catecholamines, attracted much attention as versatile coatings that can be used to cover the surface of almost any material with a conformal layer of adjustable thickness ranging from a few to about 100 nm.

GKB40 (40% Pt supported on Graphitized Ketjen black (GKB)) was coated with a thin film of PDA at different deposition times and calcined. GKB40, PDA1/GKB40 and PDA24/GKB40 electrocatalysts were investigated and evaluated in terms of their surface morphology, mass composition and structural changes using High Resolution Transmission Electron Microscopy (HRTEM), Thermogravimetric Analysis (TGA), Fourier Transmission Infrared Spectroscopy (FTIR) analysis respectively. The electrochemical activity, kinetics, and durability towards the

ORR were studied using a rotating disc electrode (RDE) and cyclic voltammetry (CV). The nanoparticles were well dispersed and found to be in the range of 3-5 nm. TGA was performed on the PDA coated catalysts which were coated for 1 hr before being calcined (PDA1/GKB40), samples coated for 24hrs (PDA24/GKB40) to estimate the amount of PDA deposited and whether the calcination degraded the catalyst. Approximately 20% of PDA material was found to be deposited on PDA24/GKB40 catalysts, which degraded during oxidation at much lower temperature as compared to uncoated GKB40 catalyst. After calcination the mass loading of Pt catalyst remaining in all the samples was determined and GKB40 commercial was observed to have approximately 3% less in Pt mass composition as compared to PDA coated GK40 catalysts.

The synthesized PDA coated catalyst presented with improved activity towards ORR and durability, having greater mass and area specific activities and lower overpotential as compared to GKB40 commercial catalyst. A remarkable increase in corrosion resistance during durability cycling treatment was observed in the PDA/GKB40, shown by the slower ECSA decay due to carbon support degradation that causes less Pt loss as compared to commercial GKB40.

The results presented here suggest that the studied PDA coating material are suitable to prepare Pt catalysts supported on graphitized Ketjen black, increasing their activity toward the ORR and durability. PDA/GKB40 are therefore good candidates to be employed as cathodes in proton exchange membrane fuel cells.

ACKNOWLEDGEMENT

Firstly, I would like to give glory to Almighty God for granting my desire and giving me the strength to pursue my MSc, it is only by His grace, I could not have done this without Him.

Secondary, I would like to express my sincerest appreciation to my supervisor, Prof. Lindiwe Khotseng, thank you so much for giving me this opportunity to further my studies and career. I know this has been a long journey for both of us. You put up with me when I could not juggle between my life outside school and studies yet you continue to support me tirelessly even when I was slacking. Your patience and kindness cannot go unappreciated.

To my co-supervisor, Dr. Jessica Chamier, I cannot thank you enough, for helping me see this project through. Thank you for always pushing me to do the best I can with your consistent guidance and tremendous support throughout my research period and during the preparation of this thesis.

I would also like to extend my appreciation to UWC electrocatalysts Group for their continuous guidance and support from the very beginning till the end, words cannot express how much I appreciate your physical and moral support. This project would also not have been possible without the support of the UCT HySA catalysis technical development team, special thank you to Ziyanda Jabe, Firdaus Hendricks, Joe Itota, Nomxolisi Dywili and Bettina Kaine for their tremendous amount of effort put into assisting me with electrochemistry and physical characterization. Another special thank you to Dr Rissa Niyobugingo, a former UCT student for proofreading and reviewing my thesis.

I would also like to express my gratitude to HySA and TESP for the financial support.

Finally, I would like to thank my friends and family for their continued support and encouragement, without which this project would not have been possible.

TABLE OF CONTENTS

KEYWORDS	ii
DECLARATION	iii
ABSTRACT.....	iv
ACKNOWLEDGEMENT	vi
TABLE OF CONTENTS.....	vii
LIST OF FIGURES	ix
LIST OF TABLES	x
LIST OF ABBREVIATIONS.....	xi
CHAPTER ONE	1
INTRODUCTION.....	1
1.1 BACKGROUND	1
1.2 PURPOSE OF THE STUDY	3
1.3 AIM AND OBJECTIVES OF THE STUDY	4
1.4 SCOPE OF THE STUDY.....	5
CHAPTER TWO	6
LITERATURE REVIEW.....	6
2.1 OVERVIEW OF FUEL CELLS.....	6
2.2 TYPES OF FUEL CELLS.....	7
2.2.1 Alkaline Fuel Cell.....	8
2.2.2 Direct Methanol Fuel Cell	9
2.2.3 Molten Carbonate Fuel Cell	9
2.2.4 Phosphoric Acid Fuel Cells	10
2.2.5 Solid Oxide Fuel Cells.....	10



2.2.6 Proton Exchange Membrane Fuel Cells	11
2.3 UNDERSTANDING THE FUEL CELL TECHNOLOGY	11
2.4 FUNDAMENTALS OF PEM FUEL CELLS	12
2.5 GENERAL WORKING PRINCIPLE OF PEMFC	16
2.6 CATALYSTS FOR FUEL CELLS	19
2.6.1 Oxygen Reduction Reaction	18
2.6.2 Catalyst for Oxygen Reduction Reaction	20
2.6.3 Catalyst Supports	21
2.7 CHALLENGES FACING THE USE OF PEMFCs	22
2.7.1 Factors affecting durability of PEMFCs	23
2.7.1.1 <i>Catalysts Degradation</i>	25
2.7.1.2 <i>Carbon Support Degradation</i>	26
2.8 MITIGATION OF DEGRADATION	27
2.10 HYPOTHESIS	30
CHAPTER THREE	31
EXPERIMENTAL METHODOLOGY	31
3.1 MATERIALS AND REAGENTS	31
3.2 SYNTHESIS AND EXPERIMENTAL PROCEDURE	31
3.2.1 Preparation of Polydopamine thin film on GKB and supported Platinum catalyst	31
3.3 CHARACTERIZATION TECHNIQUES	32
3.3.1 Physical Characterization	32
3.3.1.1 <i>Fourier Transform Infrared Spectroscopy</i>	32
3.3.1.2 <i>High Resolution Transmission Electron Microscopy</i>	33
3.3.1.3 <i>Thermogravimetric Analysis</i>	33
3.3.2 Electrochemical Characterization	33
CHAPTER FOUR	38
RESULTS AND DISCUSSIONS	38
CHAPTER FIVE	58
CONCLUSIONS AND RECOMMENDATIONS	58
REFERENCES	60

LIST OF FIGURES

Figure 1: Design of a proton exchange fuel cell	12
Figure 2: The Membrane electrode assembly of PEMFC	13
Figure 3: The components of a single cell	14
Figure 4: Working principle of PEMFC	17
Figure 5. Schematic representation of the oxygen reduction reaction (ORR) mechanism by direct pathway (A: adsorption parallel to the surface) and indirect pathway (B: adsorption perpendicular to the surface)	18
Figure 6: Structure of Polydopamine	29
Figure 7: FTIR spectra of uncoated material GKB(A) and GKB40(D) and after coating with PDA at different deposition time, B) PDA1/GKB (B), PDA24/GKB(C), PDA1/GKB40 (E) and PDA24/GKB40 (F).....	40
Figure 8: TGA results comparison of GKB, GKB40 and PDA deposited on both GKB and GKB40 at 1hr and 24hrs deposition time under Nitrogen atmosphere.....	42
Figure 9: TGA results comparison of bare GKB, GKB40 and PDA deposited on GKB and GKB40 at 1hr and 24hrs deposition time in air to determine loading.	44
Figure 10: HRTEM images of A) GKB40 commercial, B) PDA1/GKB40 and C) PDA24/GKB40 (electro-catalysts observed at higher magnification (50nm) and the corresponding images of a, b, and c at high magnification (10nm).....	47
Figure 11: Particle size distribution histograms determined from HRTEM images of A) GKB40 Commercial B) PDA1/GKB40 and C) PDA24/GKB40 electro-catalysts.....	48
Figure 12: Presents cyclic voltammograms of the synthesized electrocatalyst of PDA supported on GKB40 compared to GKB40 commercial electrocatalyst in 0.1M HClO ₄ at 20mV/s.....	50

Figure 13: Polarization curves comparison of the ORR performed on GKB40 Commercial , PDA1/GKB40 and PDA24/GKB40 electrocatalysts in O₂ saturated 0.1M HClO₄ at a sweep rate of 20mV/s, rotated at 1600rpm, at room temperature.....52

Figure 14: Mass transfer polarization curves for the ORR on GKB40 Commercial and PDA1/GKB40, PDA25/GKB40 electro-catalysts in O₂ saturated 0.5M H₂SO₄ at a sweep rate of 20mV/s, rotating velocity of 1600rpm, at room temperature.53

Figure 15: Cyclic voltammograms of GKB40, PDA1/GKB40 and PDA24/GKB40 catalysts before and after the cycling.....55

Figure 16: The ECSA% determined after every 100 cycles until 5000 cycles for commercial GKB40, PDA1/GKB40 and PDA24/GKB40 in 0.1 M HClO₄.....56



LIST OF TABLES

Table 1: Comparison of the five main types of Fuel Cells.....8

Table 2. Electro-catalysts synthesized with descriptions.....32

Table 3: Shows the total weight percentage of carbonaceous materials after decomposition of inorganic substances in GKB, GKB40 materials before and after PDA deposition at 1hr and 24hrs deposition time, performed in Nitrogen (N₂) atmosphere.....43

Table 4: Shows the total weight percentage composition of inorganic material after decomposition of organic substances in GKB and GKB40 materials before and after PDA deposition at 1hr and 24 hrs deposition time performed under Oxygen atmosphere.45

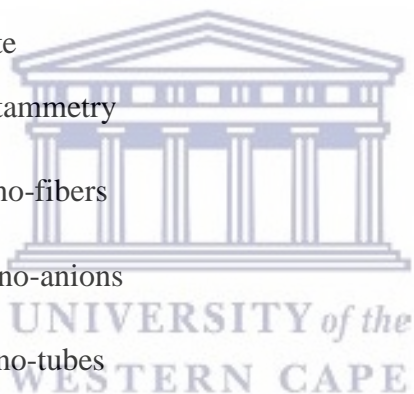
Table 5: Electrochemical surface area of GKB40 and PDA coated electro-catalysts50

Table 6: The Mass specific, Area-specific and Tafel slope activities current at half reaction ($i=0.9V$) of LSV curve of GKB40, PDA1/GKB40 and PDA24/GKB40 at 1600rpm.....53

Table 7: The ECSA loss determined after 5000 cycles of GKB40, PDA1/GKB40 and PDA24/GKB40.....56

LIST OF ABBREVIATIONS

AFCs:	Alkaline Fuel Cells
BP:	Bipolar Plate
CV:	Cyclic Voltammetry
CNFs:	Carbon Nano-fibers
CNOs:	Carbon Nano-anions
CNTs:	Carbon nano-tubes
DAFCs:	Direct Alcohol Fuel Cells
DEFC:	Direct Ethanol Fuel Cells Direct
DFT:	Discrete Fourier Transform
DMFC:	Methanol Fuel Cells
DOE:	Department of Energy
EELS:	Electron Energy Loss System
EIS:	Electrochemical Impedance Spectroscopy
ECSA:	Electrochemical Surface Area
EMU:	Electron Microscope Unit



EXAFS:	Extended X-ray Absorption Fine Structure
GDL:	Gas Diffusion Layer
GKB:	Graphitized Ketjen Black
GKB40:	40% Platinum on Graphitized Ketjen Black
HRTEM:	High Resolution Transmission Electron Microscopy
HOR:	Hydrogen Oxidation Reaction
FTIR:	Fourier Transform Infra-Red Spectroscopy
MCFs:	Molten Carbonate Fuel Cells
MEA:	Membrane Electrode Assembly
OMCS:	Ordered Mesoporous Carbon Spheres
ORR:	Oxidation Reduction Reaction
PANI:	Polyaniline
PAFCs:	Phosphoric Acid Fuel Cells
PDA:	Polydopamine
PDA/GKB:	Polydopamine on Graphitized Ketjen Black
PDA/ GKB40: Black	Polydopamine coated on 40% Platinum supported on Graphitized Ketjen Black
PEMFCs:	Polymer Electrolyte Membrane Fuel Cells
PGC:	Porous Graphitic Carbon
PGMs:	Platinum Group Metals
PPY:	Polypyrrole
PTEE:	Polytetrafluoroethylene

Pt:	Platinum
rGO:	Reduced Graphene
SOFCs:	Solid Oxide Fuel Cells
SSOFCs:	Symmetrical Solid Oxide Fuel Cells
TGA:	Thermogravimetric Analysis



CHAPTER ONE

INTRODUCTION

1.1 BACKGROUND

The need for energy and its related services to satisfy human social and economic development, welfare and health is increasing. Securing energy supply and curbing energy contribution to climate change are two over-riding challenges for the energy sector on a road to a sustainable future. An estimated 1.4 billion people in the world lack access to electricity, while 85% of them live in rural areas. As a result of this, the number of rural communities relying on the traditional use of biomass is projected to rise from 2.7 billion today to 2.8 billion in 2030 [1].

The world is largely dependent on fossil fuel energy such as oil, gas and coal providing 80 % of energy produced, with renewable energy 13.5 % and nuclear energy supplying 6.5 % of the remaining energy [1]. This large amount of energy consumed has major environmental impacts with the fossil fuels responsible for about 70-75 % of greenhouse gases which contribute to global warming [2]. The current energy supplies are unable to cope with the rapidly increasing energy demand and the emission regulations are changing and will create constraints on energy production. Alternative energy production methods have been considered which will be able to provide for the increasing energy demand while decreasing the impact on the environment.

Research into alternate sources of energy dates back to the late 90's when severe price hikes in oil shocked the world. It is evidential in literature that replacing fossil fuel-based energy sources with renewable energy sources, which includes: bioenergy, direct solar energy, geothermal energy, hydropower, wind and ocean energy (tide and wave), would gradually help the world achieve the idea of sustainability. In 2012 renewable energy sources supplied 22% of the world energy generation, which was not possible a decade before that [3].

A fuel cell is an energy device that converts chemical energy into electricity by oxidizing the fuel. Hydrogen has a high-power density and produces water as the only emission when used as a fuel

[4]. Hydrogen fuel cells work by combining hydrogen (H_2) fuel with oxygen (O_2) to produce electricity through a chemical reaction, generating water and heat as byproducts.

Hydrogen energy has been widely recognized as the most promising alternative sustainable energy source for the future. Hydrogen, like electricity, is a carrier of energy which can deliver a substantial amount of energy. The chemical energy available in hydrogen can be converted into mechanical energy either by burning hydrogen in internal combustion engines or through a chemical reaction in a fuel cell. As the world attempts to combat climate change, hydrogen fuel cells offer emission-free energy with low to zero pollutants. At present, the most suitable fuel cell being developed for transport, stationary and portable fuel cell applications is the proton-exchange membrane fuel cell [5].

This research focuses on the Polymer Electrolyte Membrane Fuel Cells also known as Proton Exchange Membrane Fuel Cells (PEMFCs) which are clean and efficient energy systems. PEMFCs are well suited to be a power source by virtue of their energy conversion efficiency, relatively simple and low weight design, environmentally friendly nature, and high energy and power densities compared to other fuel cell types [4]. The efficiency can reach as much as 60% in electrical energy conversion and an overall 80% in the cogeneration of electrical and thermal energies. Additionally, fuel cells can significantly reduce (by more than 90%) or even eliminate pollution- such as in the case of hydrogen-fuelled PEMFCs where the water forms as a non-polluting by-product, which can further be reused as potable water [6]. Use of the PEMFCs can also eliminate the emission of greenhouse gases, if the hydrogen gas is produced through water electrolysis driven by renewable energy, and not generated by burning fossil fuels. As a consequence, avoiding the need for the usage of conventional carbon-based fuels (coal, oil and gas) can significantly decrease economic dependence on oil producing countries and, therefore, also provide greater security of energy supply for the user nation [6].

However, despite the considerable advantages related with the use of fuel cells, they also show serious drawbacks. Switching from fossil fuels to fuel cells comes with its own challenges. Two major challenges towards the commercialization of PEMFCs are cost and durability. These challenges may be overcome with more advancements and developments in fuel cell technology, materials and component design.

Most fuel cells currently use Platinum group metals (PGMs), in the form of nanoparticles dispersed on carbon black support), as catalysts for the hydrogen oxidation reaction (HOR) and oxygen reduction reaction (ORR). The ORR occurring at the cathode is about 6 orders of magnitude slower than the HOR on the anode and thus limits performance. As a result, more PGMs are required for the cathode which increases raw material cost. This is a renowned challenge. Consequently, a considerable amount of research and development efforts are aimed at improving cathode catalysts towards the ORR [7].

Significant progress has been made in PEMFCs on materials, design, manufacturing, and application. However, durability remains a major challenge for large scale commercialization. A great number of parameters influence the performance, degradation, and durability of PEMFCs. Carbon has been widely used as support material for catalysts in PEMFC because of its high surface area onto which small metals can be deposited. Despite its widespread use as a catalyst support, carbon is very susceptible to corrosion [8]. Carbon support corrosion is the major contributing factor of catalyst layer degradation in PEMFCs. It has been reported that catalysts supported on carbon black gradually aggregate during long term cell operation, which reduces the ECSA, leading to irreversible performance losses [9].

Taking a step towards successful commercialization requires ORR electrocatalysts that can meet performance targets, are low in cost and are highly durable. Currently not all proposed approaches meet these demands. This study will focus on improving the durability of the supported Platinum catalyst by means of material modification. This encompasses a mitigation strategy in which the surface of the carbon support is chemical modified to reduce the effect of carbon degradation.

1.2 PURPOSE OF THE STUDY

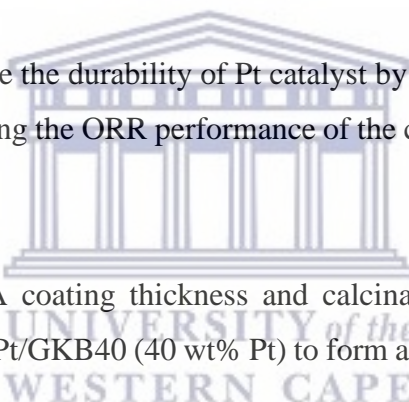
In PEMFC technological development, there are two major challenges which obstruct its pathway to commercialization; durability and cost. Recent advances in PEMFC systems showed the most common fuel cell catalysts to be platinum (Pt) (or platinum alloys) supported by carbon with high surface area in both the cathode and anode [1]. However, carbon is very susceptible to corrosion and results in lower durability of Pt supported catalysts. To reduce the effect of carbon degradation,

mitigation strategies such as material modification are used which change the chemical nature of the support.

This study will introduce the use of a polydopamine thin film as a catalyst coating to reduce the effect of support degradation, increasing the durability of the platinum catalyst. Polydopamine (PDA), has attracted much attention as versatile surface coatings on a host of materials with a conformal layer of adjustable thickness ranging from a few to about 100 nm [10,11]. Polydopamine can form a thin protective barrier (carbon layer) against harsh pH environments on the catalyst surface which improves the durability of the catalyst [12].

1.3 AIM AND OBJECTIVES OF THE STUDY

The aim of the study is to improve the durability of Pt catalyst by coating the catalyst with a layer of PDA film without compromising the ORR performance of the catalyst. To achieve this goal the following objectives are set:

- 
- Optimization of the PDA coating thickness and calcination conditions on Graphitized Ketjen Black (GKB) and Pt/GKB40 (40 wt% Pt) to form a thin amorphous carbon layer on the catalyst surface.
 - Physical characterization of the coated catalysts using high resolution transmission electron microscopy (HRTEM), thermogravimetric analysis (TGA), Fourier Transmission Infrared Spectroscopy (FTIR) analysis respectively.
 - To determine the impact of the PDA surface layer on the electrochemical surface area, the oxidation reduction reaction (ORR) activity and catalyst electrochemical durability.

1.4 LAYOUT OF THE THESIS

This thesis is constructed as follows:

Chapter 1: Prepares the readers for the thesis by providing background overview on the world's energy demands and the current energy supply shortages. Fuel cells are introduced as a promising energy source for a sustainable future supply. The importance of ORR catalysts as part of fuel cells studies is explained. A summary of the aim and objectives of the experimental study is presented.

Chapter 2: Provides a literature survey on fuel cells mainly focusing on the activity and stability of ORR catalyst in PEMFCs. This section will detail relevant literature on the problem statement which will then be used to support the work presented in this thesis.

Chapter 3: Describes the experimental methods and techniques used in this study. This includes details on the experimental procedures used in polydopamine deposition onto the support material and the relevant characterization techniques. This chapter further describes the preparation of the catalysts for electrochemical characterization.

Chapter 4: Discusses physiochemical characterization of PDA-GKB, Pt/GKB and PDA-Pt/GKB including FTIR, TGA and HRTEM. This section is followed by the results and discussion on the electrochemical characterization of the catalysts using a three-electrode cell. The catalyst activities towards the ORR and their electrochemical durability are compared.

Chapter 5: Provides the conclusions drawn from this study and recommendations for future work.

CHAPTER TWO

LITERATURE REVIEW

This Chapter presents a literature survey and background study for the project based on the Polymer Electrolyte Membrane Fuel Cell (PEMFC) electrocatalysts and their durability. The various types of fuel cells and differences are discussed in brief and a detailed analysis of the PEMFC type is the represented, detailing relevant literature on the problem statement which will then be used to support the work presented in this thesis. Furthermore, a detailed description of PEMFC catalysts degradation and the associated mitigation strategies currently implemented is represented.

2.1 OVERVIEW OF FUEL CELLS

A fuel cell is a device which converts chemical energy from a fuel into electricity through a chemical reaction with oxygen as an oxidizing agent and will continue to produce electricity for as long as the fuel and oxidant inputs are supplied. Fuel cells and batteries have similarities because both rely on the electrochemical nature of the power generation process except that a fuel cell does not need recharging as the fuel is constantly being supplied. Some of the characteristics associated to these devices are its silent operation without vibration, inherent modularity allowing to a simple construction and a diverse range of applications in portable devices, stationary units and transportation [13]. The fuel cell operates quietly and efficiently, and when hydrogen is used as fuel, it produces only power, heat and water. Therefore, a fuel cell has low emissions and provides a cleaner and more flexible chemical-to-electrical energy conversion than that offered by fossil fuel combustion. In this sense, it is important to highlight that combustion of fossil fuels has increased air pollution and the emission of greenhouse gasses such as CO₂, leading to climate change, ozone depletion and acid rain [6, 14].

The first fuel cell device was developed by Sir William Robert Grove in 1838, this device combined hydrogen and oxygen to produce electricity and was named a gas battery. Later, this device was known as fuel cell [15]. In 1959, Francis Thomas Bacon presented the first fully-operational fuel cell [13, 14]. Although fuel cells were invented in the middle of the 19th century,

they didn't find the first application until space exploration in the 1960's. Since then, the development of fuel cell technology has gone through several cycles of intense activity, each followed by a period of reduced interest. However, during the past two decades, a confluence of driving forces has created a sustained and significant world-wide effort to develop fuel cell materials and fuel cell systems [16].

2.2 TYPES OF FUEL CELLS

A fuel cell is an electrochemical device that converts the chemical energy embedded in a fuel into electrical energy through a chemical reaction with an oxidizing agent such as oxygen [29]. This conversion will continue to produce electricity for as long as the fuel and oxidant inputs are supplied. The fuel cells are classified according to the name of the fuel they use. The hydrogen fuel is the widely used fuel in fuel cells.

There are different types of fuel cells. They are divided into:

- low temperature fuel cell systems (Proton Exchange Membrane Fuel cell, Direct Methanol Fuel Cell, Alkaline Fuel Cell) and
- high temperature fuel cell systems (Molten Carbonate Fuel Cell, Solid Oxide Fuel Cell, Phosphoric acid fuel cell).

Table 1 compares the differences of the main different types of fuel cells that exists with the type of electrolyte they use, the temperature they are operated, its power density and efficiency followed by a brief description of those fuel cell types. [17].

This research focuses mainly on one type of low temperature fuel cells namely, proton exchange membrane fuel cell (PEMFC).

Table 1: Comparison of the five main types of Fuel Cells

Fuel cell Type	Operating Temperature (°C)	Transported ion	Membrane used	Power density mW/cm²	Fuel Cell efficiency
Polymer electrolyte membrane fuel cell (PEMFC)	50-80	H ⁺	Polymeric membrane	350	45-60
Alkaline fuel cell (AFC)	60-80	OH ⁻	Aqueous alkaline solution	100-200	40-60
Phosphoric acid fuel cell (PAFC)	150-200	H ⁺	Molten phosphoric acid	200	55
Molten carbonate fuel cell (MCFC)	600-700	CO ₃ ²⁻	Molten alkaline carbonate	100	60-65
Solid oxide fuel cell (SOFC)	800-1000	O ²⁻	Ceramics	240	55-65

2.2.1 Alkaline Fuel Cell

The alkaline fuel cell (AFC) was the first fuel cell technology to be put into practical service and make the generation of electricity from hydrogen feasible. Starting with applications in space the alkaline cell provided high-energy conversion efficiency with no moving parts and high reliability. AFCs were used as the basis for the first experiments with vehicular applications of fuel cells, starting with a farm tractor in the late 1950's equipped with an Allis Chalmers. However, despite its early success and leadership role in fuel cell technology, AFCs have fallen out of favour with the research community and have been eclipsed by the rapid development of PEMFC as the technology of choice for vehicular applications [18].

2.2.2 Direct Methanol Fuel Cell

Direct methanol fuel cell (DMFC) is considered as a highly promising power source. It is based on polymer electrolytes membrane (PEM) fuel cell technology. In contrast to the established hydrogen fuel cell technology, the DMFC allows the direct electrochemical oxidation of methanol to carbon dioxide under generation of electric energy. It possesses a number of advantages such as a liquid fuel, quick refuelling, low cost of methanol and the compact cell design making it suitable for various stationary and portable applications [19]. DMFCs are also environmentally friendly. Although carbon dioxide is produced, there is no production of sulfur or nitrogen oxides. Advantages of the DMFC include easy storage of the high-energy density liquid fuel and the simple reactor design without fuel reforming, as necessary to feed classical hydrogen fuel cells [19]. The development of commercial DMFCs has nevertheless been hindered by some important issues. The most important are the low power density caused by the slow electrochemical oxidation of methanol and methanol crossover through PEM, which is responsible for inhibiting the activity of the cathode catalyst. The fuel cell system has to cope with highly dynamic operating conditions. So far, most research work published in the literature is restricted to steady-state investigations [20].

2.2.3 Molten Carbonate Fuel Cell

Molten carbonate fuel cells (MCFC) have emerged as the most promising high temperature hydrogen fuel cell technologies [21]. They have attracted significant attention of many communities because of the potential contribution to the development of a sustainable society powered by unconventional, distributed clean energy sources. MCFC generate power via conversion of chemical energy of gaseous fuel (hydrogen, hydrogen-rich mixtures or hydrocarbons including biofuels into electricity through electrochemical reactions [22,23]. These electrochemical reactions require specifically designed catalysts (electrodes) in terms of their microstructure and chemical composition that govern physio-chemical phenomena related to the mass transfer properties and catalytic activity. MCFC materials should also possess high temperature and chemical stability in molten salt environments. However, using molten salt electrolytes (carbonates) is considered very promising from the point of sustainability as it

becomes possible to use MCFCs in processes that incorporate carbon cycle, and CO₂ vaporization or capture and separation to reduce CO₂ emission into the atmosphere [21,22].

2.2.4 Phosphoric Acid Fuel Cells

In the wake of the emerging importance of fuel cell-based energy generation using hydrogen as raw material, it becomes imperative to improve the real-life performance of fuel cell systems. There are various types of fuel cell among which phosphoric acid fuel cell (PAFC) represents the most mature technology [22]. This type of fuel cell uses phosphoric acid as the electrolyte, contained within a ceramic matrix such as silicon carbide or glass mat. PAFC has the most extensive track record for operational experience of any fuel cell technologies [24]. PAFC system can operate at a temperature up to 190°C and consequently less sensitive to carbon monoxide poisoning of the Pt catalyst compared to PEM fuel cell. Apart from the catalyst, the other components used in PAFC are mainly made of graphite and carbon. All these factors make PAFC a versatile member of the hydrogen-oxygen fuel cell family. However, the major drawback of PAFC is the crossover of the gases through the electrolyte and drying and flooding of electrolyte [23].

2.2.5 Solid Oxide Fuel Cells

Production of high-efficiency electrical energy with low waste heat has been the main concerns of researchers in recent decades. Solid oxide fuel cells (SOFCs) assigned to be the most effective method for the conversion of fuel chemical energy into electrical power.

SOFCs have been extensively explored as an eco-friendly technology for the production of electrical energy via electrochemical reaction between oxidant and fuel. The three key components of which a fuel cell is composed of are; the cathode where reduction of oxygen takes place to produce ions, the electrolyte solution for an ion migration and the anode where these ions react with fuel to produce electricity and other by-products [25]. Recently, symmetrical solid oxide fuel cells (SSOFCs) have drawn wide attention due to its diverse industrial applications. SSOFCs are utilizing the same material for both the cathode and anode. Possible coke formation and Sulfur poisoning at the anode can be easily eliminated by alternating the gas flow without causing damage to the cell and doubling the life-span of fuel cell. Reduction in fabrication cost can be seen because

of the same composition of cathode and anode which lets them fired in a single step. Therefore, finding an efficient and suitable electrode materials for SSOFC is restrictive and extensively studied. An efficient SSOFC electrode material should fulfil certain criteria's which includes; good structural stability and chemical compatibility with electrolyte both in oxidizing and reducing condition, appropriate electro catalytic activity for hydrogen oxidation reaction [25].

2.2.6 Proton Exchange Membrane Fuel Cells

This project investigates activities associated with low temperature polymer electrolyte membrane fuel cells (PEMFCs). PEMFCs are a clean and efficient energy system and are well suited to be a power source by virtue of their energy conversion efficiency, relatively simple design, environmentally friendly nature, high energy and power densities. Its relatively low temperature allows for quick start-ups and suitability for discontinuous operation and zero emission [26]. The use of polymer electrolyte membrane resolves limiting requirements faced by other types of fuel cells, such as the need for pure fuels [27]. PEMFCs are expected to become the most promising and clean energy converters for automotive, stationary, and portable applications. Moreover, they can be made light-weight and therefore the leading fuel cell technology for handling technologies (e.g. forklifts) and transport (e.g. cars, trains etc.). Consequently, PEMFCs have increasingly been cited by governments as a possible pathway to the reduction of greenhouse gas emissions [24,28].

2.3 UNDERSTANDING THE FUEL CELL TECHNOLOGY

The fuel cell consists of three basic components, the anode which oxidizes the fuel into protons and electrons, cathode where oxygen is reduced and an electrolyte or membrane that allows charges to move between the electrodes. The electrochemical reactions are enabled using a catalyst [30,31] . The electrons and protons are drawn from the anode to the cathode, producing direct current electricity and water. Fuel cells come in a variety of sizes and produce very small amounts of electricity, about 0.7 V and so are placed in a series or parallel circuits called stacks, to increase the voltage and current output to meet an application's power generation requirements [32]. The

energy efficiency of a fuel cell is generally between 40-60%, or up to 85% efficient if waste heat is captured for use. Figure 1 shows a schematic diagram of a fuel cell [32].

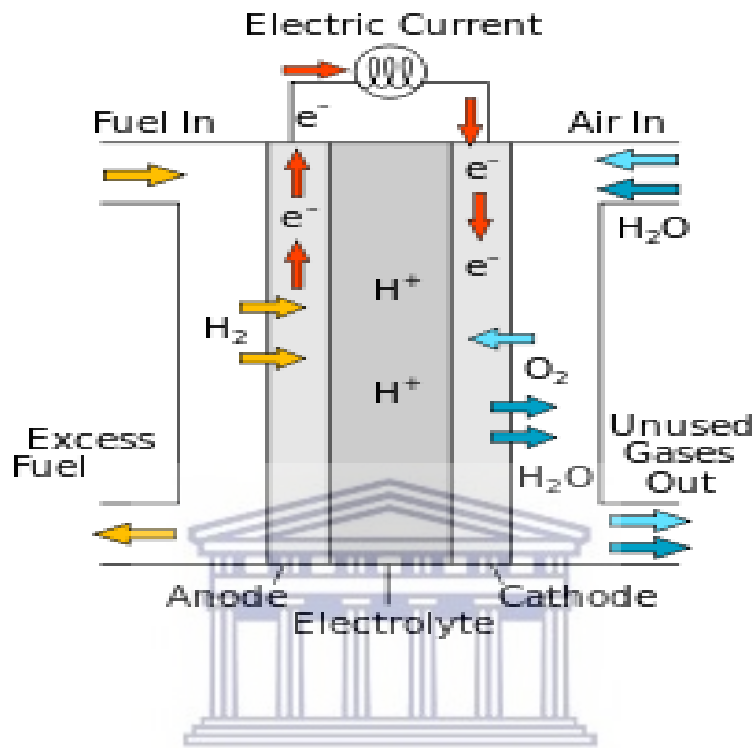


Figure 1: Design of a proton exchange fuel cell [32].

Fuel cells are galvanic cells in which the Gibbs free energy of a chemical reaction is converted into work via an electrical current. In PEMFCs, hydrogen gas dissociates into protons (H^+) and electrons (e^-) at the anode. The electrons pass through an external circuit/load producing electricity while the H^+ ions move across the proton-conducting membrane. On reaching the cathode, these electrons and protons react with the supplied oxygen to form water, which is the product of the fuel cell [30].

2.4 FUNDAMENTAL COMPONENTS OF PEM FUEL CELLS

PEMFCs are made from several layers of different materials. The structure and the components of a PEM fuel cell are described below.

The most important part of a PEMFC is the membrane electrode assembly (MEA). The MEA consists of five layers: the polymer electrolyte membrane (PEM), two catalyst layers and two gas diffusion layers [32]. The PEM, which separates the anode and the cathode compartment, ideally allows for proton transport only. The anodic and cathodic electrochemical reactions take place within the associated catalyst layers directly attached to the surface of the PEM. The diffusion layers on either side of the MEA distribute the reactant gasses and provide for good electrical contact with the catalyst layers [36]. Figure 2 below represents a typical structure of an MEA.

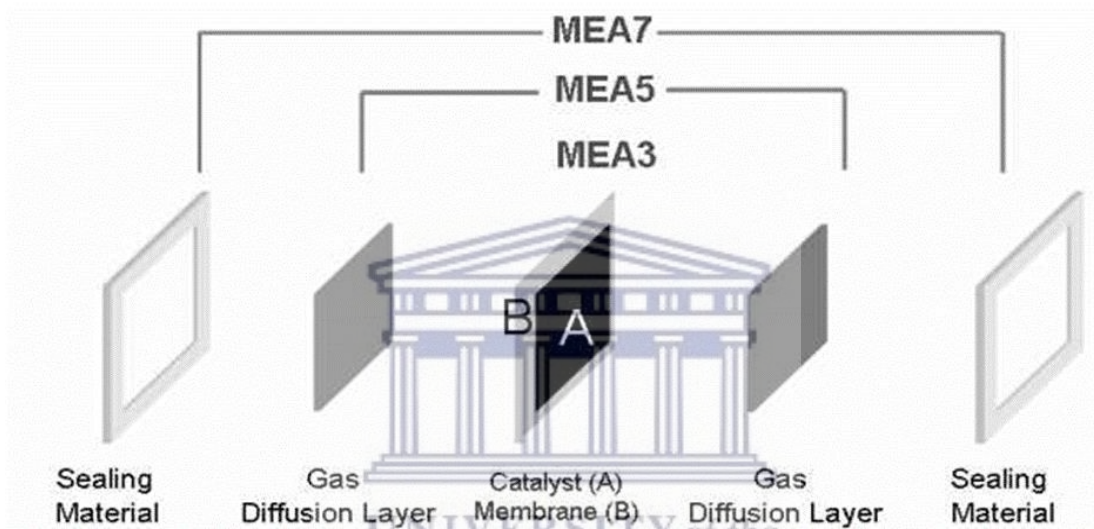


Figure 2: The Membrane electrode assembly of PEMFC [36].

Hardware components used to incorporate an MEA into a fuel cell include gaskets, which provide a seal around the MEA to prevent leakage of gases, and bipolar plates, which are used to assemble individual PEM fuel cells into a fuel cell stack and provide channels for the gaseous fuel and air.

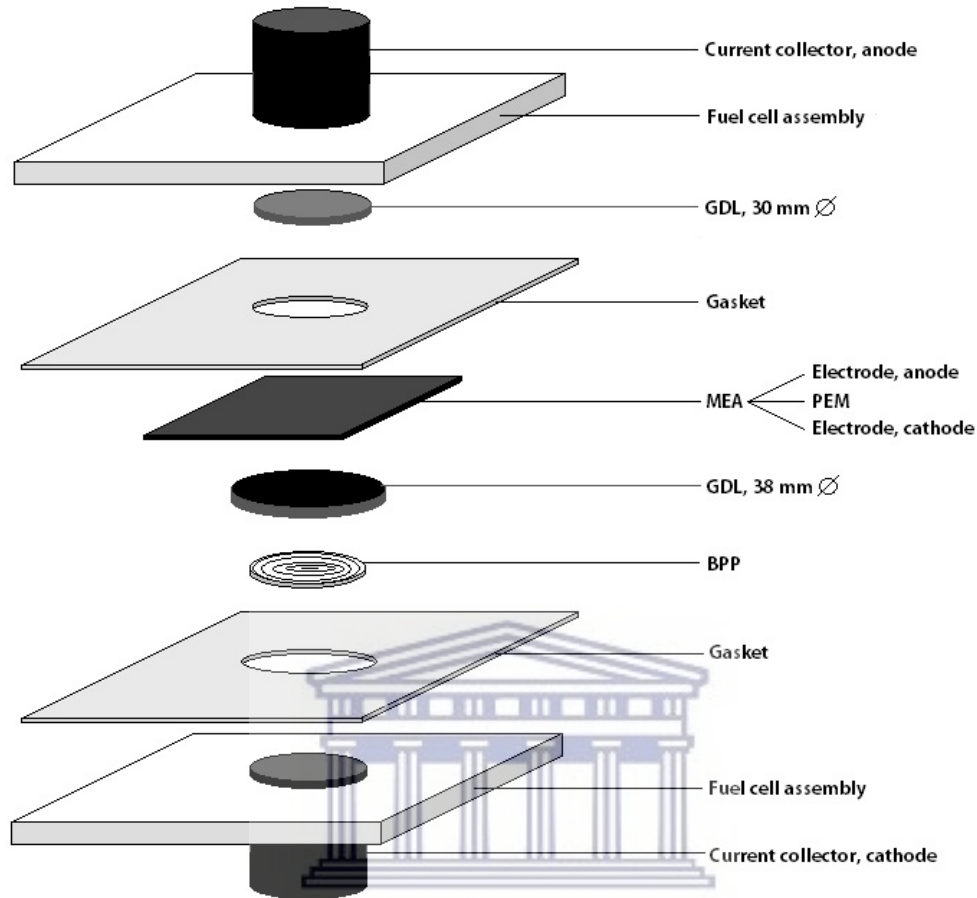


Figure 3: The components of a single cell [36].

2.4.1 Gas Diffusion Layer

The GDLs adjacent to the catalyst layers facilitate transport of reactants into the catalyst layer, as well as the removal of product water. Each GDL is typically composed of a sheet of carbon paper in which the carbon fibers are partially coated with polytetrafluoroethylene (PTFE) to form hydrophobic pores which prevents excessive water build-up. Gases diffuse rapidly through the pores in the GDL [33]. In many cases, the inner surface of the GDL is coated with a thin layer of high-surface-area carbon mixed with PTFE, called the microporous layer. The microporous layer can help adjust the balance between water retention (needed to maintain membrane conductivity) and water release (needed to keep the pores open so hydrogen and oxygen can diffuse into the electrodes [33]).

2.4.2 Bipolar Plates

The MEA is sandwiched between two bipolar plates. These plates, which may be made of metal, carbon, or composites, provide the electrical conduction and physical strength to the cell. The surfaces of the plates typically contain a flow field, which is a set of channels machined or stamped into the plate to allow gases to flow over the MEA [33].

2.4.3 Proton exchange membrane

PEM materials can conduct protons to maintain the ionic conductivity. In addition to the high ion conductivity, the membrane should be durable, robust and resistant to chemical attack. For PEMFCs, which operate below 100° C, sulfonated polymers such as Nafion (Dupont) are the most used material. The sulfonated polymers are comprised of perfluorinated back-bones and sulfonated side-chains. The perfluoroethylene is responsible for the chemical stability while the function of sulfonated side-chains is to aggregate and facilitate hydration [34].

2.4.4 Gaskets

Sealing gaskets in PEMFCs are placed between bipolar plates and the MEA. The gaskets are added around the edges of the MEA to make a gas-tight seal. The main functions of the gaskets are to prevent the leaking of reactant gases and coolants inside the cell. In addition, they also work as electrical insulators between the parts they separate. Gaskets are generally made of polymeric materials [35,36].

2.4.5 Catalyst Layer

There is a catalyst layer on either side of the PEM—the anode and the cathode layer respectively. The function of catalyst layer is to initiate the dissociation of the hydrogen on the anode, and for accelerating the oxygen reduction reaction (ORR) on the cathode. Conventional catalyst layers include nanometer-sized particles of platinum dispersed on a high-surface-area carbon support. This supported platinum catalyst is mixed with an ion-conducting polymer (ionomer) and sandwiched between the membrane and the GDLs. On the anode, the platinum catalyst enables hydrogen molecules to be split into protons and electrons [31]. The electrons produced on the anode side travel through an external circuit to produce the current while the protons traverse the membrane to the cathode side of the membrane, and combine with oxygen and the electrons

arriving from the external circuit [34]. The platinum catalyst enables oxygen reduction by reacting with the protons generated by the anode, producing heat and water [31]. The ionomer mixed into the catalyst layers allows the protons to travel through these layers.

2.5 GENERAL WORKING PRINCIPLE OF PEMFC

Fuel cells are galvanic cells in which the Gibbs free energy of a chemical reaction is converted into work via an electrical current [37]. The basic principle of the PEMFC is the conversion of chemical energy to electrical energy using a complex reaction where the reactants H_2 and O_2 undergo several catalyzed reaction steps to eventually form the product H_2O . During the reaction, heat is formed which is then released at the cathode [31].

Hydrogen gas enter at the anode while pure O_2 or air is fed at the cathode. At the anode, Hydrogen gas is oxidized and dissociates into protons (H^+) and electrons (e^-) ions. The electrons pass through an external circuit/load producing electricity while the H^+ ions are transported from the anode through a polymer electrolyte membrane to the cathode. At the cathode, O_2 react with H^+ ions and electrons in a 3-phase zone to form H_2O and heat is released. Only in this 3-phase zone consisting of the reactant gas, the liquid electrolyte and the solid electrode catalyst is the reaction between H_2 and O_2 possible [38].

This process is illustrated in Fig.4. Half-cell reactions and the total reaction of the PEM fuel cell are given as follows.

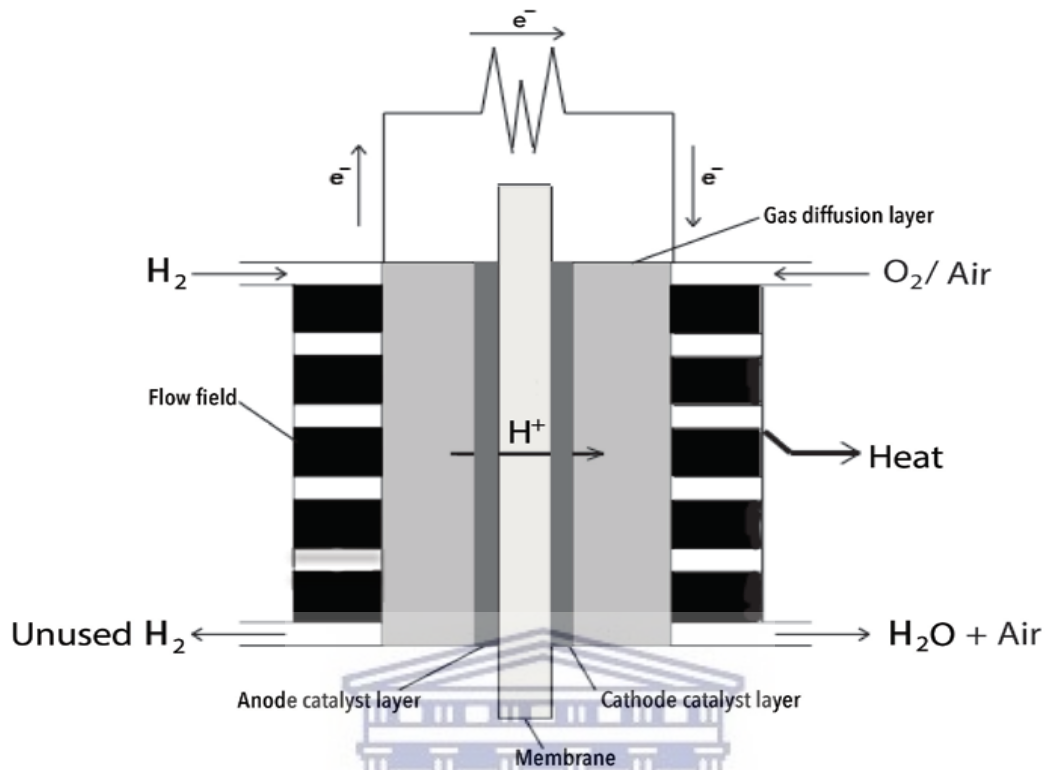
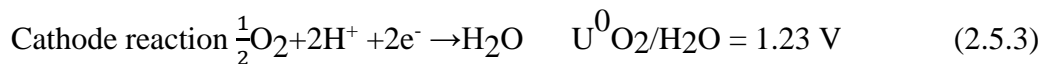


Figure 4: Working principle of PEMFC [38].



The protons (H^+) are generally solvated in water molecules. This solvated state of protons is called the hydronium ion and is represented as H_3O^+ . The half-cell reactions exhibit standard potentials of 0.0 V for the hydrogen oxidation ($U^0_{\text{H}_2/\text{H}^+}$) and 1.23 V for the oxygen reduction ($U^0_{\text{O}_2/\text{H}_2\text{O}}$). This results in a standard reversible cell potential of 1.23 V. The oxygen stream at the cathode side is usually air, and about 77% by mass of it is nitrogen [39].

2.5.1 Oxygen Reduction Reaction

Despite the advantage of high conversion, high energy density and low carbon footprint, fuel cells are fully commercially viable primarily due to the slow kinetics of the oxygen reduction reaction (ORR) occurring at the cathode [42].

A high over potential is required for the ORR to occur in low temperature fuel cells [43]. The mechanism of the ORR on Pt is sensitive to the properties of the surface and the presence of other adsorbed species on the catalyst. To increase the performance of the ORR, the mechanism and kinetics of the ORR have been studied on a great variety of electrode materials and electrolytes.

ORR is a multielectron reaction that may include a number of elementary steps involving different reaction intermediates. The ORR can take place through two pathways, (Figure 5) that is the four-electron pathway which is the electro-reduction of oxygen to water and there's also the two-electron transfer which is the electro-reduction of oxygen to hydrogen peroxide [44-46]. The first pathway is the direct four-electron pathway and it takes place via the reaction pathway above (see reaction 2.5.3).

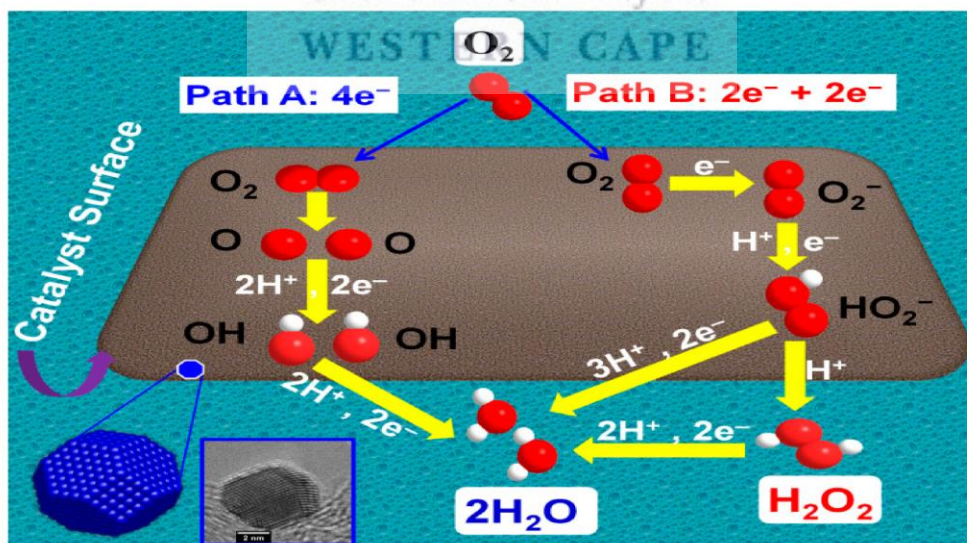
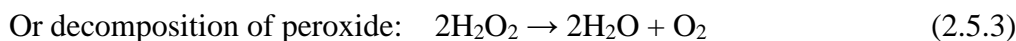
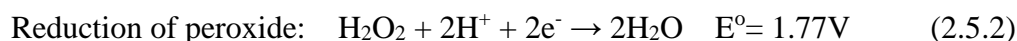


Figure 5. Schematic representation of the oxygen reduction reaction (ORR) mechanism by direct pathway (A: adsorption parallel to the surface) and indirect pathway (B: adsorption perpendicular to the surface) [43].

The second pathway is the peroxide pathway, which is a two-step process involving the two-electron electrochemical reaction creating hydrogen peroxide (see reaction 2.5.1) and then the subsequent two-electron decomposition (see reaction 2.5.3) or reduction (see reaction 2.5.2) of peroxide to water or hydroxide ions. The formation of hydrogen peroxide takes place when the oxygen reduction is not completed. The following steps below represent the reaction pathway:



This combined four-electron pathway results in the presence of hydrogen peroxide in the solution, before it is either reduced or decomposed into hydroxide ions or water [44]. The peroxide that is produced is low in efficiency and corrosive.

According to Figure 5, the ORR starts with the adsorption of oxygen on the surface of two adjacent platinum atoms. Once the water is formed, this is desorbed from the catalyst surface [48].

Due to the slow kinetics of the oxygen reduction reaction, catalysts are used to increase the reaction rate. It has been found that platinum has the highest catalytic activity, which can be increased by reducing the particle size and supporting it onto a conductive material [43]. The Pt catalyst is the widely used catalyst for ORR but it is expensive.

2.6 CATALYSTS FOR FUEL CELLS

Fuel cells consist of two electrodes. These electrodes contain catalysts that speed up electrochemical reaction which occur on these electrode surfaces. Research done on platinum alloys and other noble metals found platinum to be the most widely used catalyst. There are many factors that affect the rate of the reaction such as bigger particle size, lower surface area, low temperature, low pH etc.

A catalyst is a compound that increases the rate of a reaction but is not consumed during the overall reaction. The catalyst's role in a reaction is to make the rate of the reaction fast such as to lower the energy needed for the reaction to take place. Catalysts are classified as heterogeneous and homogeneous. A heterogeneous catalyst does not dissolve in a solution, and hence the catalyst is in a different phase separate from that in which the reaction occurs. A homogeneous catalyst dissolves in a solution. Acids, bases, enzymes and most organometallic species are used as homogeneous catalysts. The energy which is needed to initiate a reaction is called activation energy. A catalyst can lower the activation energy without itself being changed or consumed during the reaction. All catalysts operate by the same principle, that is, the activation energy of the rate-determining step must be lowered in order for a rate enhancement to occur [40].

In a fuel cell the anode catalyst oxidizes the fuel and the cathode catalyst reduces the oxygen and this results in the formation of water. The ORR has a low reaction rate due to the higher energy requirement. A catalyst is needed to lower the activation energy and increase the reaction rate [41].

2.6.1 Catalyst for Oxygen Reduction Reaction

Platinum is a silvery-white, lustrous, ductile, and malleable pure metal [49]. It is more ductile than gold, silver and copper [50,51]. Platinum does not oxidize at any temperature, although it is corroded by halogens, cyanides, sulfur, and caustic alkalis. It is insoluble in hydrochloric acid, but dissolves in hot aqua regia to form chloroplatinic acid, H_2PtCl_6 [52]. The metal has an excellent resistance to corrosion and high temperature and has stable electrical properties. It is used for industrial applications [53]. Platinum is mostly used as a catalyst in chemical reactions, as platinum black. This metal also catalyzes the decomposition of hydrogen peroxide into water and oxygen gas [54]. Pt is used as a catalyst in fuel cells for both electrodes. The cathodic ORR is significantly slower than the HOR therefore requires higher amounts of Pt [55]. The Pt catalyst is supported to increase the electrochemical surface area, and therefore the reaction rates.

Consequently, the state-of-the-art commercially available catalysts use highly dispersed Pt or Pt-alloy nanoparticles as the active catalyst material in fuel cell applications. To increase the surface area and reduce the Pt loading, Pt/M-alloy catalysts, where M is a base metal (M= Co, Ni, Cr, Fe)

are used. Some of these Pt-based binary alloy catalysts (Pt-Co, Pt-Cr and Pt-Ni) were prepared and compared with Pt in ORR studies [56,57,58]. Pt-alone and Pt-based alloy electro-catalysts showed increasing specific activities with decreasing surface area. This indicates that oxygen reduction on platinum surface is a structure-sensitive reaction and the Pt-based alloy catalysts showed significantly higher specific activities than Pt-alone catalysts with the same surface area [59]. This comes from the reduced Pt–Pt neighbouring distance as the catalysts were alloyed. The reduced Pt–Pt neighbouring distance is favourable for the adsorption of oxygen [59].

It is also observed that alloys with smaller Pt-Pt distance than in pure Pt usually have higher ORR activity. Although, the exact cause of such improvements is elusive, it is generally accepted that introduction of the second metal (M) favourably alters the electronic structure of surface Pt atoms in a way that enhances its ORR activity. Thus, depending on the application, it may be possible to use tailor made catalysts. But this usually involves a trade-off between activity and durability [55]. A major challenge of Pt catalyst, is catalyst layer degradation mainly caused by loss in the electrochemical surface area of Pt or Pt alloys. The main degradation mechanisms can be broadly identified as (i) Pt dissolution; (ii) Pt nanoparticle migration and agglomeration; and (iii) carbon corrosion [60]. These processes are interrelated and will be discussed further in (Section 2.8).

Research is being done to find ways of reducing the cost of the catalyst in the MEA. The move from Pt black to carbon supported Pt catalysts has significantly cut Pt requirements. Typical loadings in the electrode today are about 0.4-0.8 mg Pt/cm², which is significantly lower than 25mg/cm² with early Pt black catalysts [61].

2.6.2 Catalyst Supports

Platinum based catalysts are deposited on catalyst supports to enhance their surface area [62]. A catalyst support is the material, usually a solid with a high surface area, to which a catalyst is affixed [63]. The catalyst supports prevent the electro-catalysts from aggregation but also play a significant role in transporting the electrons generated from and consumed by the electrical reactions [64]. It has been reported that catalyst supports play a significant role in the performance and durability of electro-catalysts. An ideal catalyst support should have the following properties:

- High surface area to improve the catalytic dispersion
- High electrochemical and thermal stability
- Low combustion reactivity,
- High conductivity
- High corrosion resistance
- Low cost

Currently, the most popular support material is porous carbon black but there are various studies conducted on other types of carbon support material, e.g. carbon nanotubes and non-carbon materials e.g. metal oxides etc. [65]. Although some metal oxide and ceramic supports show encouraging results, most possess low surface areas resulting in low catalyst dispersion and consequently, low electrochemical activity [66]. Carbon black remains the ideal support due to low costs, however, they undergo corrosion during operation [65].

For this study graphitized Ketjen black was used as catalyst support. Graphitized carbon supports have been gaining more attention due to increased corrosion resistance, high surface area, chemical stability and superior electrical conductivity [67]. Graphitic content has also been found to be more robust and resistance towards carbon corrosion, Pt on reinforced graphite only had a 25% loss in ECSA compared to 60% and 80% loss observed by Pt on Vulcan and Pt on high-surface area carbon respectively [68].

2.7 CHALLENGES FACING THE USE OF PEMFCs

PEMFCs face major challenges, including cost and durability of PEMFCs catalyst. The catalysts are prone to chemical, mechanical and thermal degradation during its lifespan which results in a voltage and performance decline [69]. The challenges of durability and cost are the main barriers to mass commercialization of fuel cell technology.

Due to the finite availability of PGMs, the materials used reflect in the cost of the fuel cell and in the context of commercialization, cost reduction is a major factor.

Increasing the durability of the fuel cell is a major drive and a growing focus to bridge the gap between the ideal and current state of fuel cell technology [70]. The life time goals for fuel cell range from approximately 5000 operating hours for vehicular applications and 40,000 for stationary applications [71]. One of the major factors effecting the durability is materials challenges such as the durability of the carbon support. Carbon corrosion of electrodes is proven to be a major cause in performance drop in fuel cell [72]. In normal operation, this degradation is not a primary cause of performance loss due to the low potential ranges (0.6-0.85V). However, during events such as start-up, shutdown and fuel cell starvation, the corrosion of the carbon support occurs rapidly due to high potential (>1.2) thereby permanently damaging the catalyst layer [73].

2.7.1 Factors affecting durability of PEMFCs

In addition to cost and performance, long term stability of the catalyst is important. Often-quoted lifetime targets for fuel cells are 5,000 h for automotive and 40,000 h for stationary applications [74]. The membrane and the catalyst must withstand these durations without significant changes in performance. The membrane may degrade over time due to attack by peroxide radicals which can form at the cathode. Presence of contaminants in the cell can accelerate the rate of peroxide generation. Contaminants such as chloride ions may also poison the Pt catalyst. Purity of fuel cell components is critical to stability, although high purity sometimes results in higher cost. The catalyst may also lose stability due to sintering of Pt particles, dissolution of Pt, and corrosion of the carbon support [74].

Significant progress has been made in PEMFCs materials, design, manufacturing, and application. However, durability remains a major challenge for large scale commercialization. While the lifetime of PEMFCs used for stationary applications has exceeded 3 years, the automotive MEAs do not meet the required Department of Energy (DOE) standards [75]. A great number of parameters influence the performance, degradation, and durability of PEMFCs. They can be attributed to operating conditions, cell design and assembly, environmental conditions, and degradation mechanisms [76].

PEM fuel cells comprise different components including the membrane, catalyst, catalyst support, GDL, bipolar plate and sealing gaskets. Each of these components can degrade or fail to function, hence resulting in the fuel cell system performance degradation with time [77].

The durability of each component can be affected by internal and external factors. These include the material properties, fuel cell operating conditions, (i.e., humidity, temperature, cell voltage) impurities or contaminants in the reactants, environmental conditions, (such as subfreezing or cold start), operation modes (e.g. start-up, shutdown, potential cycling, etc.), and the design of components and the stack. The degradation routes in a fuel cell system are interconnected and may affect multiple components. Long-term durability tests are required to assess the degradation mechanism of these components under various stress scenarios. However, it is costly and not viable to operate a fuel cell under its normal conditions for several thousand hours for those tests. Thus, accelerated test methods are implemented to obtain condensed information on the main degradation mechanisms and impacts on overall durability [77,78].

Many researchers worldwide are devoted to finding a better understanding of degradation causes and mechanisms, with early detection of the degradation symptoms [79]. Fuel cell diagnostics not only detect the symptoms, but also identify the causes and/or mechanisms, which could inform corrective actions. There are several degradation mechanisms, typical for automotive applications, such as:

- Degradation of the catalyst layer caused by carbon corrosion due to frequent starts and stops (air fuel front).
- Catalyst active area loss caused by Pt dissolution and sintering due to frequent voltage cycling.
- Catalyst active area loss due to adsorption of contaminants from the inlet gases [31].
- Mechanical degradation due to thermal and humidity cycling induced by the load profile.
- The environment in which the vehicle operates, cold and wet or dry and dusty.

Corrosion of carbon-based supports not only degrades the catalyst by lowering the electrochemical surface area (ECSA), but also has a profound effect on the electrode

morphology [33]. To decrease degradation of the catalyst, this project therefore focuses on reducing carbon corrosion.

2.7.1.1 Catalysts Degradation

In many cases, Pt catalyst degradation impacts on fuel cell durability and life span [80]. One cause of catalyst degradation is the dissolution of the platinum particles into ions. The ions either redeposit on large Pt particles or dissolve and migrate away from the catalyst layer and into nearby regions. Sustained degradation reduces the available catalyst surface in the anode and cathode resulting in loss of power.

Carbon corrosion is another degradation route in a fuel cell [79]. The carbon structure corrodes into particles that migrate into the membrane and GDL. The migrating Pt and carbon particles weaken the membrane structure as discussed above, causing irreversible structural damage ultimately resulting in tears and pinholes. Oxidation of the Pt particles may also occur which results in the formation of surface films that effectively reduce the available catalyst surface area resulting in loss of power. While oxidation of Pt reduces the surface area, it is also known to protect Pt particles beneath the oxide layer from dissolution [79].

Early empirical models attempted to capture the effect of catalyst degradation and the resultant power loss based on hours of operation. These models are incomplete and do not account for the fuel cell operational factors that results in catalyst degradation. Several models of fuel cell electrochemical interactions account for platinum catalyst degradation. They capture the physics of the rate of dissolution and oxidation of the platinum particles. These models show the significant effect of fuel cell operating voltage on catalyst degradation [79].

Pt particles supported on carbon are not stationary, but can migrate across the carbon support and agglomerates to form bigger particles, resulting in loss of active surface area. The particle growth decreases the total surface tension. Therefore, the interaction of Pt with carbon, as well as the interaction of Pt precursor with carbon during the catalyst formation, is crucial to the stability of the catalyst. Several strategies have been adopted to inhibit Pt migration and agglomeration such

as the use of stable catalyst support, and modification of Pt deposition method to enhance metal-support interaction [60].

2.7.1.2 Carbon Support Degradation

Carbon support corrosion is the major contributing factor of catalyst layer degradation in PEMFCs. Despite being the most widely used catalyst support for PEMFC, carbon support is actually thermodynamically unstable at PEMFC operating conditions. Carbon is very susceptible to corrosion. Carbon corrosion is accelerated in environment which are wet, have a low pH (<1), high temperature (50-90 °C), high oxidative potential (0.6 -1.2 V), and high oxygen concentration [47]. Oxygen atoms are being generated by the Pt catalyst and at elevated temperatures, the oxygen atoms combine with the carbon to form CO and CO₂ which leave the cell. After a significant amount of carbon is lost, the noble metal nanoparticles dislodge from the electrode or aggregate to larger particles, reducing catalytic activity, and leading to a structural collapse of the electrode [47]. Oxidation of carbon support can also lead to changes in surface, destabilizing the supported catalyst. It has been reported that during the start-up and shutdown of a fuel cell, the cathode potential can reach up to 1.5 V which significantly accelerates carbon corrosion [47].

Electrochemical carbon support corrosion proceeds as in:



The reaction is almost negligibly slow at the potential at which the fuel cell operates (< 1V) Provided it is constant throughout the operation. However, automotive PEMFC systems experience significant dynamic operating conditions involving an estimated 300,000 voltage cycles over the lifetime of a vehicle (5500 h) could result in an increase in potentials at both the anode and cathode, thus, accelerating the carbon corrosion process with detrimental effects on PEMFC performance [81].

As carbon support corrodes, Pt nanoparticles agglomerate into larger particles and/or detach from the support material, consequently reducing the electrochemical surface area (ECSA) and catalytic

activity. In the case of severe corrosion, the porous structure of the catalyst layer can be destroyed, increasing the mass transport resistance due to the blockage of gas access paths [60].

Corrosion of the carbon support also may lead to performance loss [82]. When carbon corrodes, the relative percentage of conductive material in the catalyst layer decreases. The resistance of the remaining dielectric material then dominates the cell resistance. Further, as the carbon support oxidizes, the thickness of the catalyst layer decreases, decreasing electrical contact with the current collector and increasing the cell resistance. Carbon corrosion also decreases the number of sites available to anchor platinum, resulting in metal sintering. The extent of carbon corrosion in the cell depends on the operating conditions and the specific chemistry of the support used [82].

2.8 MITIGATION OF DEGRADATION

Recent research has proposed and successfully employed several strategies to enhance catalyst durability. To mitigate or prevent the effects of fuel cell operations on the durability of the MEA, and more specifically the catalyst layer, there are two main strategies: System management strategies and materials modification [83].

System management mitigation requires the monitoring of multiple operation parameters with required sensors and feedback loops. Although costly, these strategies are approached in the balance-of-plant development and operation, and once set in place, extent for the lifetime of the fuel cell [84]. Material modifications unlike system management strategies, aim to prevent the impacts of failure events on the components. The materials contained in the components are chemically or physically modified to increase their resistance during degradation events [85].

According to the degradation mechanism of Pt/C cathode catalysts in PEMFC. Studies by Yu and Ye, 2007, proposed the following strategies towards the improvement of the catalysts stability by chemical modification: (i) building proper surface functional groups (including surface oxygen functional groups), or increasing the basic sites on carbon supports to enhance the Pt–C interaction; (ii) increasing surface stability of carbon support. Since carbon corrosion in a PEM fuel cell condition is an electrochemical process, the increasing of the hydrophobicity through proper

surface treatment of the carbon surface would be beneficial to the suppression of carbon degradation; (iii) preparing catalysts with high platinum uniformity and low platinum load [86].

Catalyst supports are one of the main factors which affect the stability of fuel cell. Increasing the graphitic degree is a valid approach to enhance the intrinsic thermal and chemical stability of carbon supports. Several advanced nanostructured carbon supports with high graphitic degree including carbon nanotubes (CNTs), carbon nanofibers (CNFs), reduced graphene oxide (rGO), ordered mesoporous carbon spheres (OMCS), and carbon nano-onions (CNOs) are more corrosion-resistant and thereby promising to substitute conventional carbon black [87]. However, highly graphitized carbon often suffers from low surface area, poor porous structure, weak PGM–support interaction, and insufficient anchoring sites, thus leading to the inhomogeneous dispersion of the supported PGM particles [88]. Appropriate surface treatment such as oxidation treatment, heteroatoms doping and polymer modification that can introduce functional groups and defect sites to the carbon supports is required to improve the interaction between PGM particles and carbon supports.

Wu et al. developed a 3D N-doped porous graphitic carbon (PGC) as durable and active support to load Pt nanoparticles, which is derived from the carbonization of polyaniline (PANI) and polypyrrole (PPy) polymer hydrogel with manganese salt as graphitized catalyst [89]. The introduction of Mn salt guarantees the high graphitization of polymer hydrogel-derived carbon prepared at a low temperature of 1100°C compared with traditional high temperature graphitized treatment requiring heating treatment up to 3000°C, which alleviates the impact of high temperature on nitrogen dopant loss and surface area decrease. EXAFS results and DFT calculations by Qiao et al., revealed that the more electronegative nitrogen doping alters the electronic state of the carbon support and Pt atoms are prone to bind with bridge sites adjacent to the N dopant much stronger than those in the pristine carbon matrix. Pt/PGC exhibited high stability in MEA under real PEMFCs working environment. In particular, the voltage loss at a current density of 1.5 A cm⁻² of MEA with Pt/PGC as cathodic catalyst was found to be only 9 mV after 5000 potential cycles from 1.0 to 1.5 V, far exceeding commercial Pt/C cathode and even the DOE durability target (<30 mV) [90]. Beyond the remarkably enhanced stability, the Pt/PGC also displays outstanding activity owing to the optimum balance between graphitization and the porous structure of the PGC support [89].

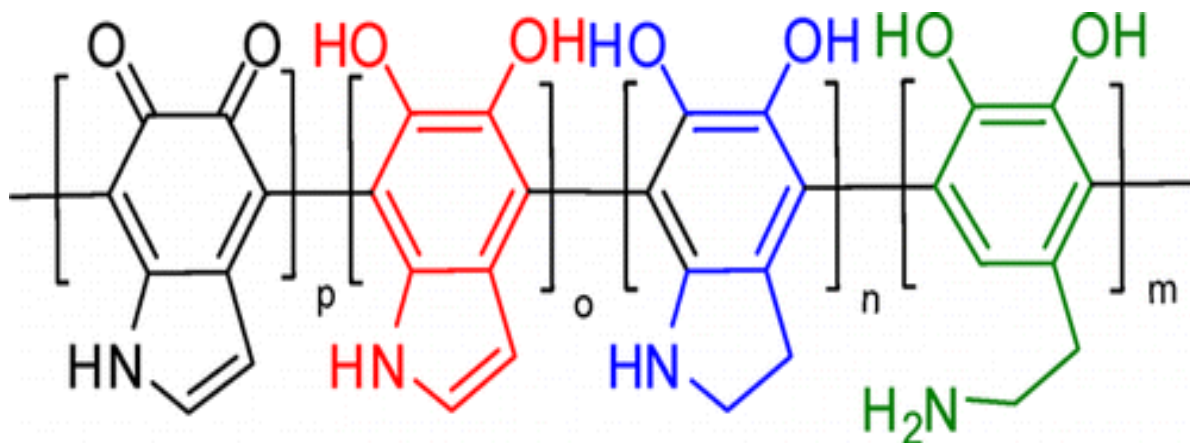


Figure 6: Structure of Polydopamine [91].

PDA, the final oxidation product of dopamine or other catecholamines, also attracted much attention as versatile surface coatings onto almost all materials with a conformal layer of adjustable thickness ranging from a few to about 100 nm [91]. This study therefore introduces the use of polydopamine (PDA) thin film as a possible corrosion resistant material to mitigate carbon corrosion in PEMFC to meet the durability and requirements.

On a simple level, PDA has long been considered as a polymer coating material inspired by nature. During the past few years, research on PDA has been directed toward the construction of smart PDA-coated functional substrates based on the inherent adhesive property of PDA. However, the function of PDA is not limited to adhesion [92].

Furthermore, PDA was previously used to develop ORR catalysts under metal and metal-free conditions [93,94]. The presence of nitrogen groups in the PDA increases the electrical conductivity while enhancing the electron affinity of the catalytic sites which facilitate adsorption of oxygen molecule, weakens the oxygen-oxygen double bond and therefore lowering the required overpotential. However, the use of PDA as a coating for ORR catalysts, in which metal is supported on carbon, has yet to be fully explored [94].

2.10 HYPOTHESIS

It is hypothesized that using PDA as a coating material on Pt electrocatalyst in PEMFCs will increase the durability of the catalyst due to its inherent adhesive property, its ability to cover the surface of almost all materials with a conformal layer of adjustable thickness. The PDA thin film can therefore serve as a corrosion resistant support material to reduce the effect of carbon support degradation, thus sustaining the durability of platinum catalyst and enhance the activity of the ORR due to its high conductivity.



CHAPTER THREE

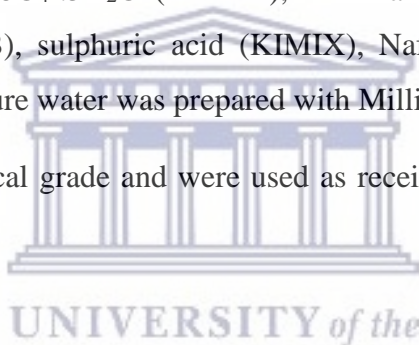
EXPERIMENTAL METHODOLOGY

The experimental procedure describes the preparation method of electro-catalysts as well as the physical and electrochemical characterization techniques used to study them.

3.1 MATERIALS AND REAGENTS

Platinum, normally 40% on Graphitized Ketjen Black (GKB40), dopamine hydrochloride (Germany), Cupric sulphate $\text{CuSO}_4 \cdot 5\text{H}_2\text{O}$ (KEMIX), Trizima base tris-Hcl (PH 8.5) (USA), Graphitized Ketjen black (GKB), sulphuric acid (KIMIX), Nafion (Alfa Aesar), isopropanol $\text{C}_3\text{H}_8\text{O}$ (Alfa Aesar) and Ultrapure water was prepared with Milli-Q system.

All the reagents were of analytical grade and were used as received from the suppliers without further purification.



3.2 SYNTHESIS AND EXPERIMENTAL PROCEDURE

3.2.1 Preparation of Polydopamine thin film on GKB and supported Platinum catalyst

To form a polydopamine (PDA) layer onto GKB and Platinum supported on Graphitized Ketjen black (GKB40) the following procedures was followed. 100 mg of GKB (or GKB40) was added to 100 ml of 30 mM of cupric sulphate. 0.1mg ml^{-1} of dopamine hydrochloride was added to 10 mM tris-HCl (pH 8.5) in 100 ml deionized water. The solutions were combined, and the mixture was stirred for 30 min at room temperature, rinsed and dried. The procedure was for 24 hours exposure time, rinsed and dried overnight in the oven at $80\text{ }^\circ\text{C}$. The dried samples of each deposition time were calcined at 400°C in N_2 for 60min. The prepared catalysts are presented in Table 2.

Table 2. Description of the synthesized catalysts

Synthesized materials	Name
1. PDA-1/GKB	PDA deposited on GKB for 60min deposition time
2. PDA-24/GKB	PDA deposited on GKB for 24hrs deposition time
3. PDA-1/GKB40	PDA coated on GKB40 for 60min deposition time
4. PDA-24/GKB40	PDA coated on GKB40 for 24hrs deposition time

3.3 CHARACTERIZATION TECHNIQUES

3.3.1 Physical Characterization

3.3.1.1 Fourier Transform Infrared Spectroscopy

FTIR spectra reveal the composition of solids, liquids, and gases. Infrared spectrum is molecular vibrational spectrum [95]. When exposed to infrared radiation, sample molecules selectively absorb radiation of unique wavelengths which causes the change of dipole moment of sample molecules. Therefore, the vibrational energy levels of sample molecules switch from ground state to excited state. The frequency of the absorption peak is decided through the vibrational energy gap. The variety of absorption peaks is associated with the wide variety of vibrational freedom of the molecule. The intensity of absorption peaks is associated to the change of dipole moment and the possibility of the transition of energy levels [96].

The FTIR analysis was used in this study to identify the functional groups and identify chemical bonds associated with polydopamine on the various surfaces

3.3.1.2 High Resolution Transmission Electron Microscopy

Transmission electron microscopy (TEM) is a microscopy technique where a beam of electrons produces a micrograph when transmitted through a specimen. A micrograph is made from the association of the electrons with the sample as the beam is transmitted through the sample. The image is then amplified and centered onto an imaging device; a fluorescent screen, a layer of photographic film, or a sensor such as a charge-coupled device. A typical TEM consists of the following components: light source, condenser lens, specimen stage, objective lens and projector lens [1].

In this study, TEM analysis was performed in the Electron Microscope Unit (EMU) at the University of Cape Town on FEI/Tecnai T20 with a high-resolution camera and electron energy loss system (EELS). A small amount of the Pt electrocatalysts synthesized was mixed with acetone and sonicated for 1min. A few drops of dispersion were deposited onto a carbon coated copper grid. The acetone was evaporated under a UV- lamp for approximately 5 min. This was performed to evaluate the distribution and particle size of the nanoparticles on GKB40.

3.3.1.3 Thermogravimetric Analysis

Thermogravimetric analysis (TGA) is the change of the mass of a sample with temperature or time during temperature rise, constant temperature or temperature reduction. The purpose is to study the thermal stability and composition of the material. A TGA consists of a sample pan that is supported by a precision balance. That pan resides in a furnace and is heated or cooled during the experiment. The mass of the sample is monitored during the experiment.

TGA was performed on an STD 560 TGA at the University of Cape Town. A small amount (2-10mg) of sample was placed in a ceramic crucible and oxidized synthetic air at 10°C per min from 25°C to 800°C. TGA was performed on GKB to establish its oxidation temperature and mass decomposition of the synthesized catalyst as well as to determine the Pt loading.

3.3.2 Electrochemical Characterization

Electrochemistry is one powerful technique to study material electron transfer properties. When electron transfer is between a substrate and a solution species, it is a heterogeneous interaction.

All electrochemical measurements were performed on a three-electrode cell using a Hg/HgSO₄ reference electrode, a Pt wire counter electrode and glassy carbon working electrode (geometric area = 0.196 cm²) working electrode on which the catalyst was studied. The electrolyte used was a 0.1 M HClO₄ prepared with Millipore deionized water and the solution was bubbled with Argon gas to remove all dissolved oxygen.

The catalyst ink was deposited onto the working electrode. To make the ink, 7.6 mg of the synthesized catalyst was made into a suspension with 40 μL of Nafion, 2.7 ml isopropanol and 7.3 ml ultrapure Millipore water. The inks were sonicated in an ultrasonic bath for 30min. Once the catalyst in the ink was adequately dispersed, 10 μL was drop cast onto a polished glassy carbon electrode with a diameter of 2.5 mm. The film was left to dry in air. To ensure consistency and reproducibility, a fresh ink was made for every batch of tests run to mitigate any settling of the catalyst in the ink. All glassware (including beakers, electrochemical cell, bubblers, etc.) were cleaned using a Nochromix bath. They were soaked overnight in the bath thereafter cleaned thoroughly using Millipore deionized water (18.2 mΩ). Once cleaned they were submerged in a 5L beaker filled with Millipore water for storage before use.

3.3.2.1 Cyclic Voltammetry

Cyclic voltammetry (CV) is used to study the reactivity of new materials or compounds and can offer information about (i) the oxidation or reduction potential, (ii) the oxidation state of the redox species, (iii) the number of electrons involved, (iv) the rate of electron transfer, (v) viable chemical processes corresponding with the electron transfer, and (vi) adsorption effects etc. [97].

In CV the voltage is swept between two values at a fixed rate, resulting in a forward and reverse scan (anodic and cathodic, respectively). CV can be used to determine the electrochemical surface area (ECSA) of an electrocatalyst, reaction kinetics and reaction mechanisms occurring on the electrode.

To condition the catalyst films, CV was scanned between 0.0 V to 1.0 V vs. RHE at 50 mV/s for 100 cycles to electrochemically clean the catalyst surface of any surface impurities. To determine

the ECSA, Cyclic voltammograms were taken in the potential range between 0.05 V and 1.2V at 20 mV/s. All the experiments were conducted in triplicates to ensure reliable and good results. The ECSA was determined using the H₂ adsorption and desorption currents on Pt under Argon purge to avoid the contribution from faradaic reactions.

The number of electrons liberated during the oxidation/reduction of hydrogen on Pt is equivalent to the number of hydrogen atoms desorbed/ adsorbed and thus the number of adsorption sites. The ECSA can then be determined using the following equation [98].

$$\text{ECSA} = \frac{Q (\mu\text{C}/\text{cm}^2)}{210 (\mu\text{C}/\text{cm}^2 \text{ Pt}) \times \text{Pt loading (gPt}/\text{cm}^2)} \quad (3.1.1)$$

210 $\mu\text{C}/\text{cm}^2\text{Pt}$ is the charge required to reduce a monolayer of protons on Pt. The total charge of ions, Q, corresponding to the hydrogen adsorption can be calculated through integration of the area where hydrogen adsorption occurs.

The total charge, Q, can be calculated using the following equation [99].

$$Q = \int_{t_1}^{t_2} I dt = \frac{1}{v_b} \int_{E_1}^{E_2} I dE \quad (3.1.2)$$

Where v_b is the scan rate, I, is the current and E, is the electrode potential. The integral was calculated using the integration tool on Excel. To avoid overestimating the total charge density attributed to electrocatalytic activity of the Pt surface, the area due to double layer charging and the hydrogen crossover currents are subtracted from the area of hydrogen adsorption. The validity of the method implies that the point where hydrogen adsorption is complete can be exactly identified, and that the coverage is completed before the rate of hydrogen evolution becomes significant [100].

To determine the ORR activity of the electrocatalysts the electrolyte was bubbled with oxygen for 30 minutes and after that the electrode was purged with oxygen while the experiment was running. CV scans were performed in an O₂-saturated electrolyte (0.1 M HClO₄) with the potential cycled between 1.2 V and 0.5 V at 20 mV/s. Polarization curves were obtained at four different rotation speeds, 400rpm, 900rpm, 1600rpm and 2500rpm by subtracting the N₂ saturated voltammogram from the O₂ -saturated voltammogram to remove any background contributions. The activity was

determined at rotational speed of 1600rpm in the same potential window. The electrochemical cell was tilted, and the working electrode rotated to remove any O₂ gas bubbles that form on the electrode surface which block the catalyst surface and effect the measurements. Kinetic ORR activity (*I_k*) was calculated for the anodic sweep curve via the following relationship:

$$I_k = \frac{I_{lim} \times I_{total}}{I_{limit} - I_{Total}} \quad (3.2.1)$$

where *I_{lim}* is the diffusion-limited current and *I_{total}* is the total current.

The parameters for determining the activity include mass activity and specific activity. All current densities were calculated from the geometric disk area. Mass activity was calculated from the equation below:

$$MA = \frac{I_k}{Pt \text{ loading}} \quad (3.2.2)$$

where MA is the mass activity in A/gPt, *I_k* is the kinetic current in A, and Pt loading is the mass of Pt in g on the electrode surface [101].

The specific activity (A/m²) is defined as:

$$SA = \frac{MA}{ESCA} \quad (3.2.3)$$

where SA is specific activity of the catalyst, MA is the mass activity A/gPt and ESCA is the electrochemical surface area in m²/g [101].

According to electrode kinetic theory [98], the kinetic current density (*j_k*) can be expressed as a Tafel form

$$n = a - \frac{2.303RT}{\alpha n F} \log j_k \quad (3.3.1)$$

where η is the overpotential, a is an exchange current density related constant, R is the gas constant, T is the temperature, F is the faraday constant, n is the electron transfer number in the determining step of the ORR, and α is the electron transfer coefficient. The plot of η and $\log j_K$ gives a linear relationship, and the slope is $2.303RT/\alpha nF$. This slope is called the Tafel slope. The higher the Tafel slope, the faster the overpotential increases with the current density. Thus, for an electrochemical reaction to obtain a high current density at low overpotentials, the reaction should exhibit a low Tafel slope.

3.2.2.2 Electrochemical durability of Carbon Support

The electrochemical durability of the supported catalyst is measured by its ability to retain its activity after being subjected to extreme potentials for long periods [102]. Several Accelerated Stress Tests (ASTs) for PEMFC components (e.g., electrocatalyst, catalyst support, membrane) have been developed by the U.S. Department of Energy (DOE), the U.S. DRIVE Fuel Cell Tech Team (FCTT), and the Japan Automobile Research Institute (JARI) to evaluate the durability of electrocatalysts [103]. In this study, CV was used to cycle and study the ECSA degradation during potential cycling [103]. The AST for carbon corrosion in this studied required the potential cycling between 1 and 1.5 V for 6000 cycles at 250 mV/s. The ECSA was recorded after every 10 cycles till 100 cycles, every 100 cycles till 1000 cycles and finally every 1000 cycles till 6000 cycles were reached. The ECSA was determined at 20mV/s between 0.05V and 1.2V.

CHAPTER FOUR

RESULTS AND DISCUSSIONS

This chapter evaluates the physical and electrochemical properties of the polydopamine coated and uncoated Pt catalysts determined through the experimental tasks formulated in the literature review and given in Chapter 3. The results in this section start with structural characterization using Fourier Transform Infrared Spectroscopy. The material composition was determined using Thermogravimetry analysis and morphological of the platinum-based catalysts was studied using high resolution Transmission Electron Microscopy. The electrochemical performance and characteristic of the catalysts were studied using cyclic voltammetry (CV) and Rotating disk electrode (RDE) techniques.

4.1 PHYSICAL CHARACTERIZATION

4.1.1 Fourier Transform Infrared Spectroscopy

All the catalysts synthesized were supported on the graphitized ketjen black (GKB), which is a unique electro-conductive carbon black with an intrinsic resistivity of about 0.01-0.1 [Ω .cm] that has received favorable evaluation for its superior performance and stability of quality, GKB has garnered high marks for providing the same level of electro-conductivity with lower loading quantity as conventional carbon black, however GKB's pore structure allows it to perform in a manner that is superior to that of other types of carbon black. The chemical structures of the untreated GKB and GKB40 and after PDA deposited on GKB and GKB40 material were studied with Fourier-Transform Infrared spectra (FTIR) to verify the surface chemical group composition and the successful modification with PDA film. The individual spectra observed are presented in Figure 7. There were no obvious absorption peaks in the wavelength region below 2000 cm^{-1} and above 3000 cm^{-1} for untreated GKB and GKB40. PDA material was then introduced onto the surface of GKB and GKB40, this was also done at different deposition times (1hr and 24hrs) to examine the time effect on the success of PDA thin film deposition onto the electrocatalysts surface material. After coating with PDA, Peaks of spectrum observed at the wavelength of 1500-1650 cm^{-1} (1hr and 24hrs deposited) and 3200-3600 cm^{-1} (24hrs deposited) indicated atomic vibration

of the N-H group hydroxyl groups in the structure. Moreover, the intense peaks below 1700 cm^{-1} are attributed to aromatic C=C and C-H bonds. And the intense peak in the regions of $1250\text{-}1310\text{ cm}^{-1}$ is attributed to C-O stretching and between $1730\text{-}1830\text{ cm}^{-1}$ is attributed to C=O stretching [104].



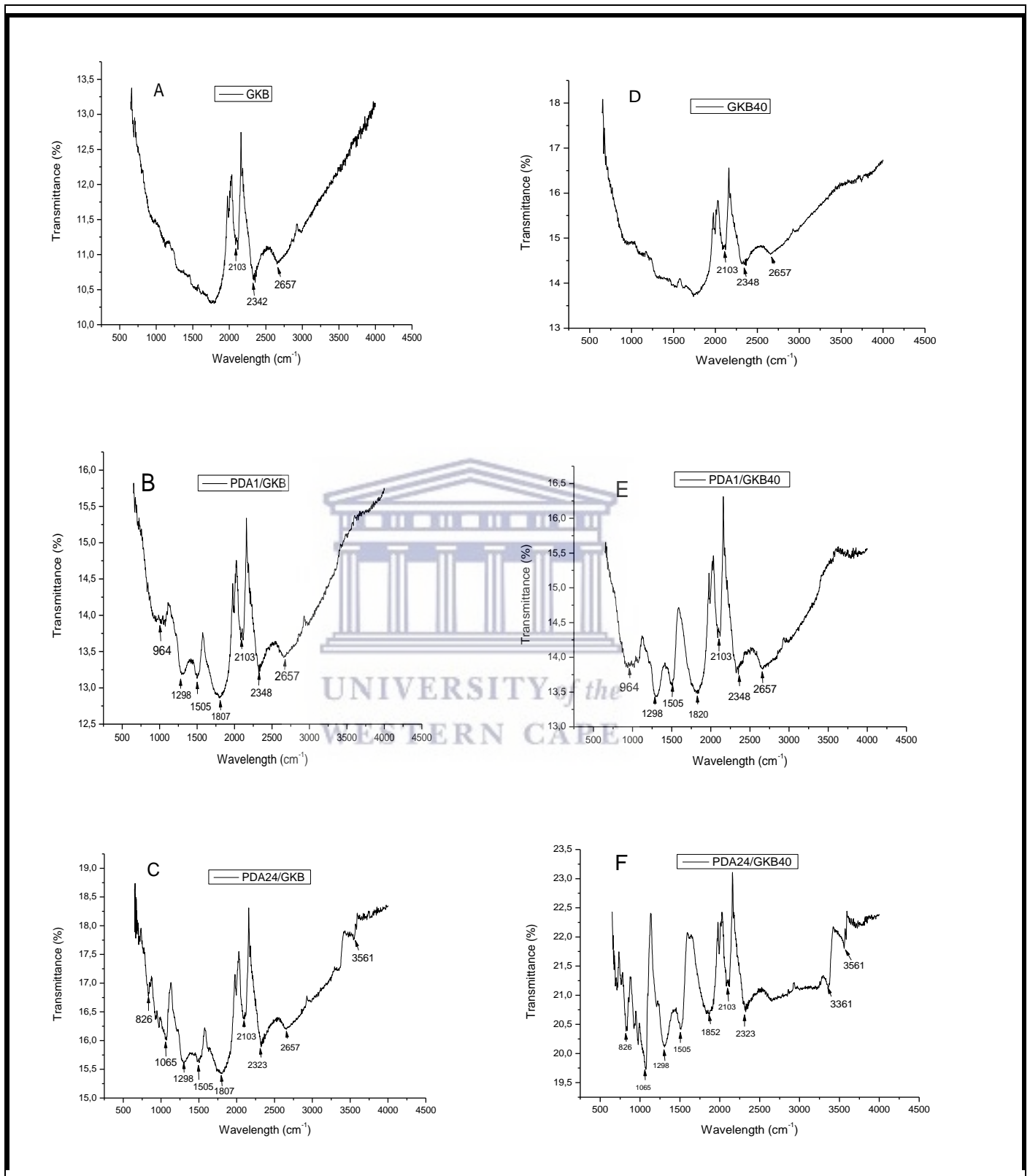
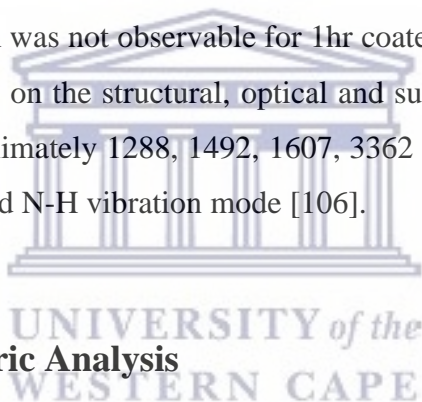


Figure 7: FTIR spectra of uncoated material GKB(A) and GKB40(D) and after coating with PDA at different deposition time, B) PDA1/GKB (B), PDA24/GKB(C), PDA1/GKB40 (E) and PDA24/GKB40 (F).

The presence of the coating layer is confirmed by the presence of increased absorbances for the PDA coated material as compared to GKB and GKB40. For GKB and GKB40 materials the only observable peaks were due to C=C=O (ketene) stretching, O=C=O (carbon dioxide) stretching and C-H (aldehyde) stretching. For the PDA coated material, the formation of PDA thin films stimulated the occurrence of new peaks after 1hr and 24hrs deposition times, the new peaks observed include C=C, C-H (aromatic) bonds, C-O (aromatic ester) stretching, C=O (acid halide) stretching, N-H (amine) vibration and O-H (hydroxyl groups). Zhao et al., study on the polydopamine-based surface modification, also found similar observations [105]. The primary difference between 1hr and 24hrs PDA coated on both GKB and GKB40 support is the peaks due to hydroxyl groups observed at the wavelength region between 3200-3600 cm^{-1} observed when PDA was coated for 24hrs which was not observable for 1hr coated. A study by Damberg et al., on the influence of PDA coating on the structural, optical and surface properties confirmed that PDA peaks are located at approximately 1288, 1492, 1607, 3362 cm^{-1} which correspond to C-O, C=N or/ and C=C and -OH or/and N-H vibration mode [106].



4.1.2. Thermogravimetric Analysis

TGA was performed on the GKB and GKB40 catalyst before and after the deposition of the PDA film to determine the amount of carbon versus Pt, and possibly the amount of PDA which was coated onto the surface of the materials as a fraction of the weight %. Under nitrogen atmosphere in Figure 8, the low-volatile processing aids (volatile material) and polymers were thermally degraded. However, the carbon material remained unchanged because of its inertness under nitrogen atmosphere. From Figure 8 for uncoated GKB and GKB40, decomposition of non-carbonaceous material starts at approximately 400°C with a gradual decrease and for PDA coated material decomposition starts at approximately 200°C with 1hr coated decomposing gradually and a drastic decomposition observed for 24hrs PDA coated material. The total % weight decomposition is reported in Table 3.

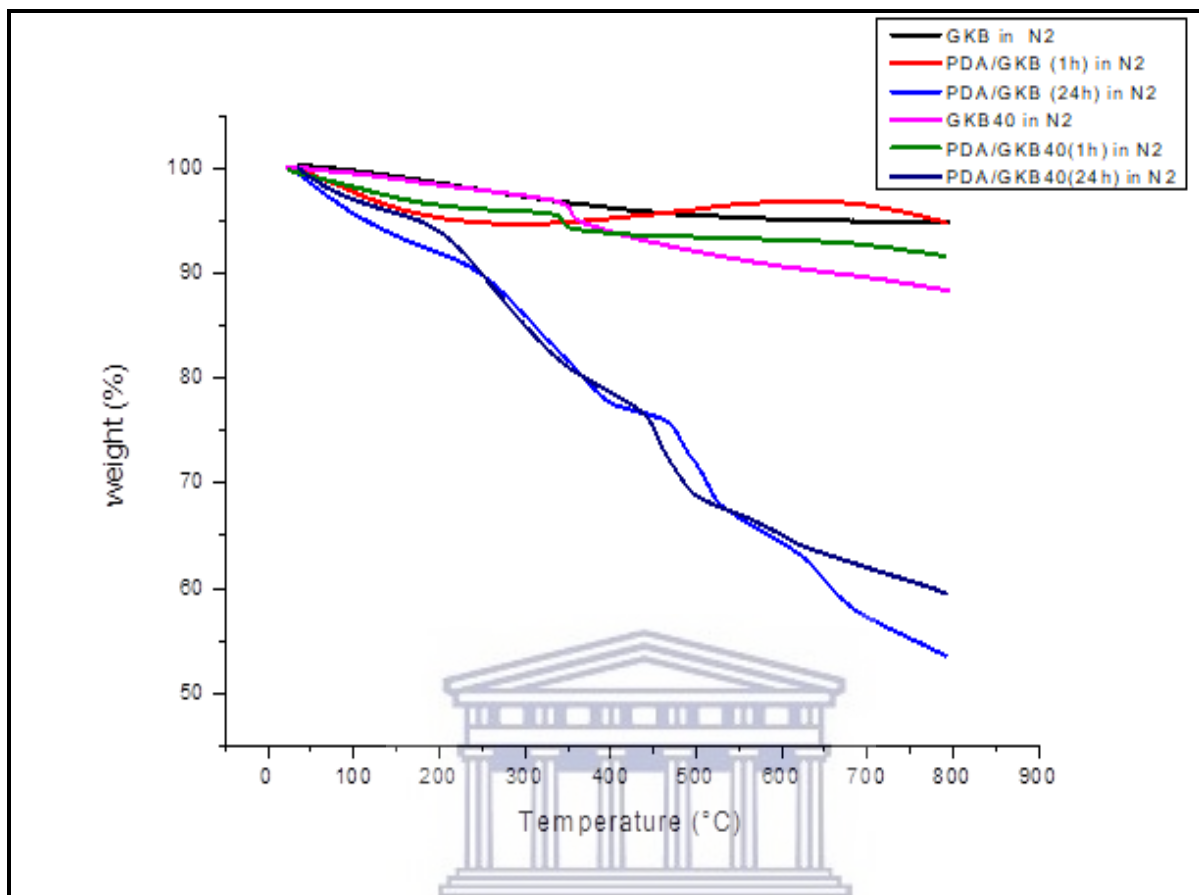


Figure 8: Comparison of TGA results obtained for GKB, GKB40 and PDA deposited on both GKB and GKB40 at 1hr and 24hrs deposition time under N₂ atmosphere.

TGA results above performed in N₂ was performed to compare the catalyst coated and uncoated by observing the temperature at which decomposition of PDA takes place. The weight loss was determined as a function of temperature. From the results in Table 3, the 1hr PDA coated material weight decreased gradually with only less than 10% decrease whereas 24hrs PDA coated material decreased drastically with more than 50% decrease in carbonaceous material. This would imply that substantially more PDA was coated onto the surface of the GKB materials after 24hrs. The results also suggest that PDA deposition for 24hrs may not be ideal since it results in far less carbonaceous material remaining for catalyst support, suggesting a decomposition of some of the carbon along with low volatile materials under N₂ atmosphere. Considering the 1hr PDA coated GKB40 material as compared to uncoated material, there is evident of a slight increase in carbonaceous material remaining of approximately 3.2% after decomposition.

Table 3: Shows the total weight percentage of carbonaceous materials after decomposition of inorganic substances in GKB, GKB40 materials before and after PDA deposition at 1hr and 24hrs deposition time, performed in Nitrogen (N₂) atmosphere.

Sample	Total weight % of degradable, volatile and polymer materials in the substance at (800 °C)	Total weight % of material at 800 °C
GKB	5.1%	94.9%
PDA1/GKB	5.5%	94.5%
PDA24/GKB	46.0%	54.0%
GKB40	11.6%	88.4%
PDA1/GKB40	8.4%	91.6%
PDA24/GKB40	35.0%	65.0%

After calcination, TGA was also performed in the air to determine the composition of PDA and final loading of Pt catalyst on the GKB support before and after PDA deposition. The TGA Thermal curve of each substance are shown in Figure 9 displayed from left to right. Thermal curves indicate initial weight loss (approx.10%) due to removal any moisture present in the sample at temperature below 200⁰C and the second degradation due to carbon oxidation of any carbonaceous material present in the sample occurred under oxygen atmosphere. The TGA shown in Figure 9, confirmed that the GKB is stable in air till around 600 °C before it begins to oxidize. When coated with Pt, GKB40, the supporting catalyst starts oxidizing at approx. 400⁰C. After coating GKB and

GKB40 with PDA films, the thermogram showed that the mass loss began at significantly lower temperatures (approx. 200°C) for 24hrs deposited compared to the uncoated GKB40 which began at (approx.400°C). The mass loss is ascribed to carbon oxidation until constant region is reached > 700 °C which reflects Pt weight percent due to the thermal stability of Pt [89]. Thermal analysis results for O₂ atmosphere are provided in Table 4.

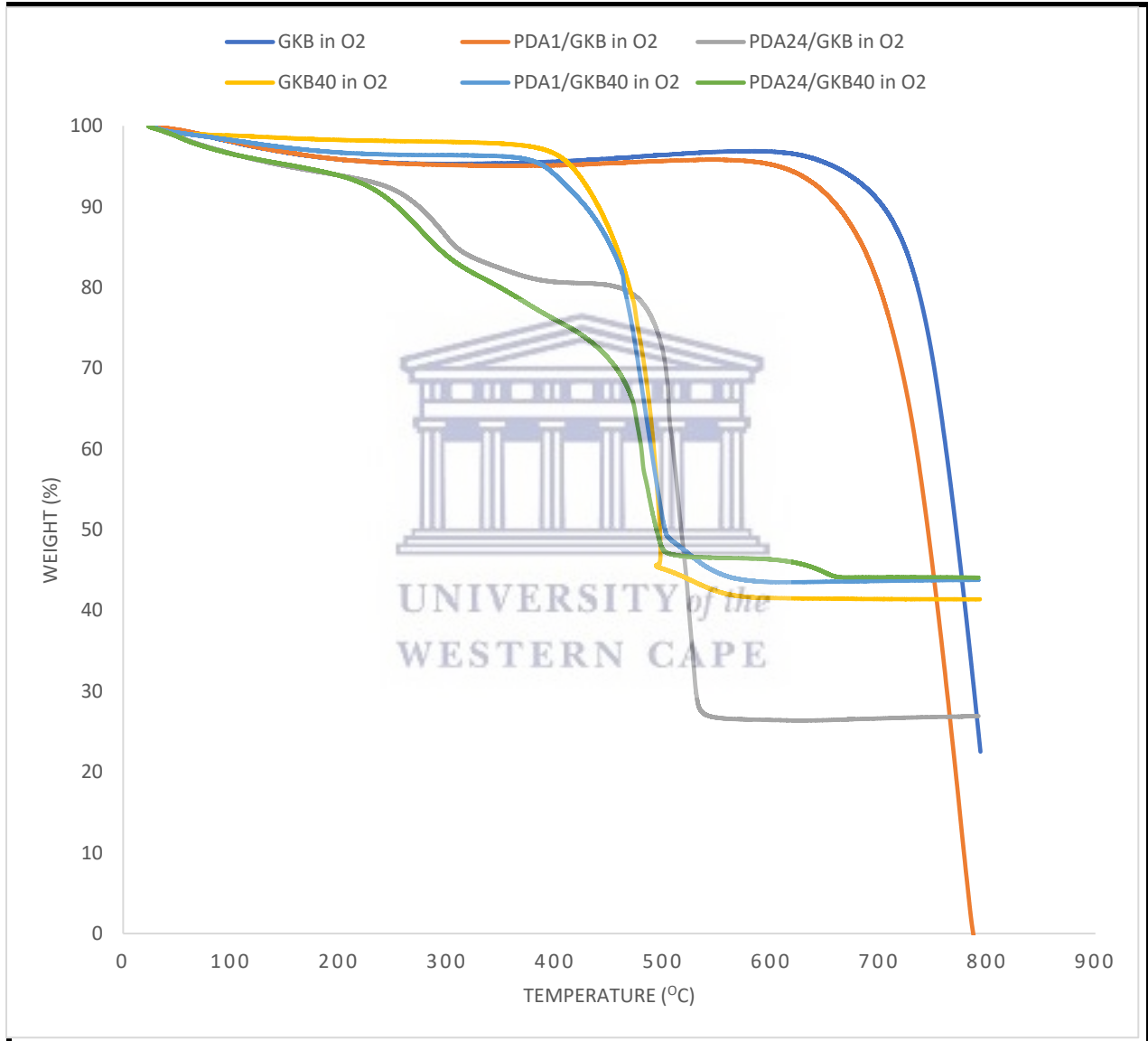


Figure 9: TGA results comparison of bare GKB, GKB40 and PDA deposited on GKB and GKB40 at 1hr and 24hrs deposition time in air to determine loading.

Table 4: The total weight percentage composition of inorganic material after decomposition of organic substances in GKB and GKB40 materials before and after PDA deposition at 1hr and 24 hrs deposition time performed under O₂ atmosphere.

Sample	Total weight % Of organic substances decomposition	% Weight composition of inorganic residue in the substances at 800 °C
Commercial GKB	78.1%	21.9%
PDA1/GKB	100.0%	0.0%
PDA24/GKB	73.1%	26.9%
Commercial GKB40	59.0%	41.0%
PDA1/GKB40	56.1%	43.9%
PDA24/GKB40	56.0%	44.0%

From the thermogravimetric results observed after calcination, the addition of PDA onto the surface of GKB and GKB40, contributed to the increase in composition of carbonaceous substance available for carbon oxidation, this is confirmed by the existence of low-temperature oxidation process observed. Approximately 20% of initial composition of PDA coated catalyst decomposed

at low temperature (approx. 200°C-400°C) due to oxidation attributed by deposition of PDA material only since GKB is only stable in the air at temperatures above 400°C before it oxidizes. The addition of PDA favored the oxidation at much lower temperature as seen in (Fig.9) leaving a stable support for the catalyst at high temperature. After degradation of organic substance, the remaining final mass loading of Pt catalyst reflected by the constant region is found to be 41% in GKB40, 44% for PDA1/GKB40 and 44% for PDA24/GKB40. PDA/GKB40 coated catalyst composition is found to be slightly high (approx.3%) compared to commercial uncoated GKB40 catalyst after calcination.

4.1.3 High Resolution Transmission Electron Microscopy

High Resolution Transmission Electron Microscopy (HRTEM) was used to study the morphology of the catalysts. It was also used to determine the particle size and the particle distribution of the catalysts on GKB after coating and calcination. Typical micrographs of TEM images are shown for GKB40, PDA1/GKB40 and PDA24/GKB40 catalysts in Figure 10. The GKB support is observed in the HRTEM images as large grey particles with small black Pt particles distributed upon them, due to the difference in mass and density. From the TEM images the respective Pt particle size histograms were determined. The average particle sizes are shown in Figure 11.

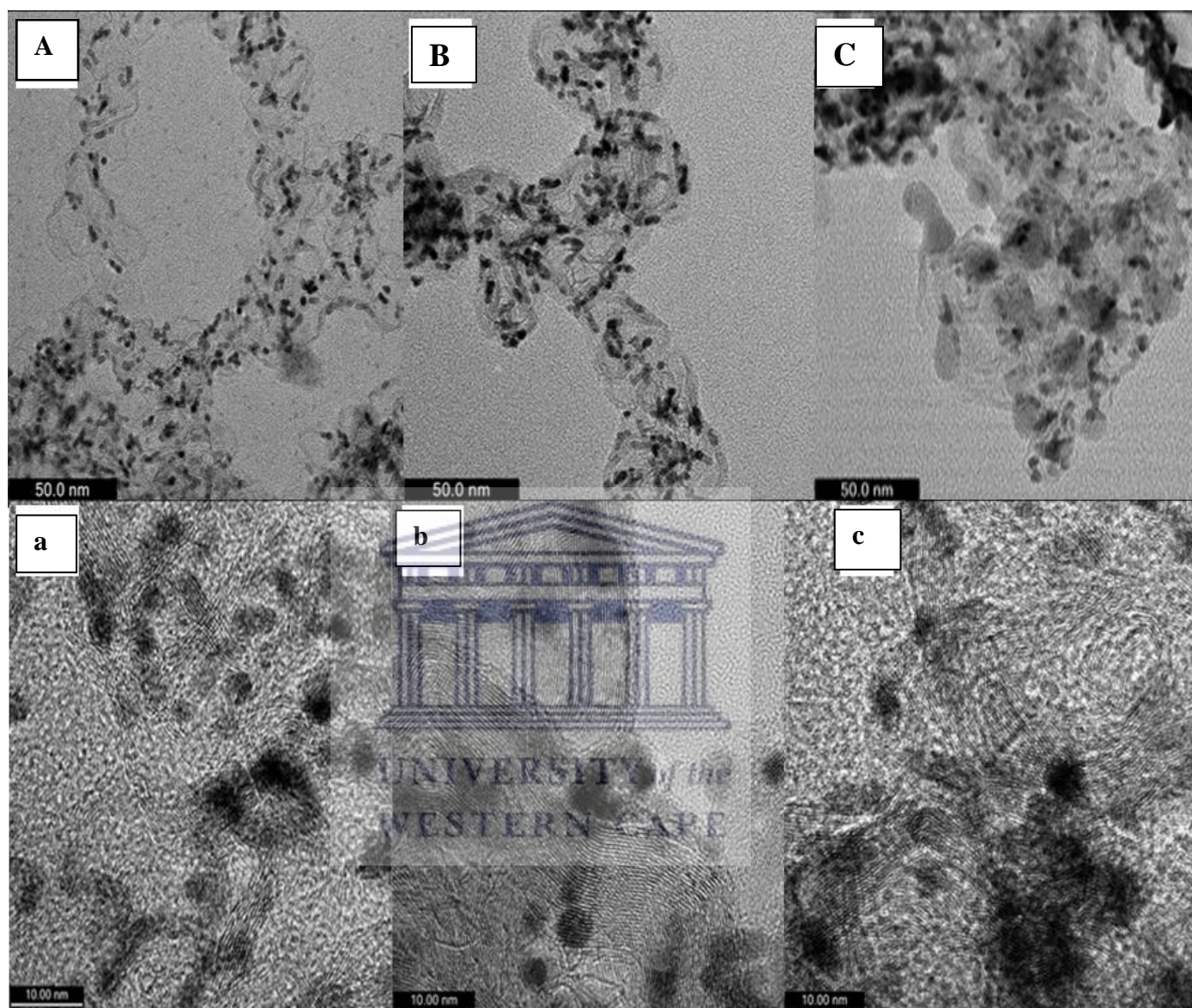


Figure 10: HRTEM images of A) GKB40 commercial, B) PDA1/GKB40 and C) PDA24/GKB40 (electro-catalysts observed at higher magnification (50nm) and the corresponding images of a, b, and c at high magnification (10nm).

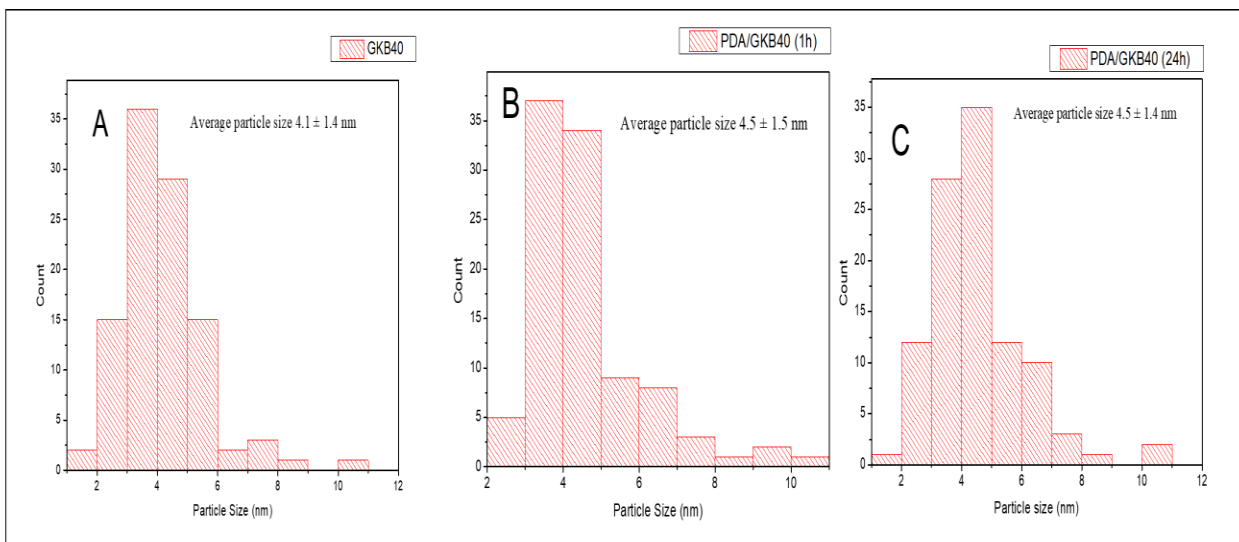


Figure 11: Particle size distribution histograms determined from HRTEM images of A) GKB40 Commercial B) PDA1/GKB40 and C) PDA24/GKB40 electro-catalysts.

From the TEM images in Figure 11, the particle size distribution (PSD), measured over 100 particles, showed an average particle size of 4.1 ± 1.4 nm for GKB40, 4.5 ± 1.5 nm for PDA1/GKB40 and 4.5 ± 1.4 nm for PDA24/GKB40. Fine particles and good metal dispersion of almost the same sizes were obtained for GKB40 and PDA coated GKB40 electrocatalysts. The sticklike carbon structure also changed for 24hrs PDA coated material which indicates carbon agglomeration. The Pt dispersion remained stable after calcination of the PDA coated catalyst. The particle size increased slightly after coating and calcination. This could be attributed to the agglomeration of the nanoparticles to form some large particles observed for PDA coated catalyst, this is supported by a study of Yu, X. and Ye., on Pt catalysts supported on the carbon material at elevated temperatures [47]. However, in this study with 80% of the particles lying in the same range of 3.0 – 5.0 nm for all the electrocatalyst characterized (seen in Figure 11). It is suggested that the polymerization of dopamine on the surface of the support material successfully formed a PDA film that stabilized the catalyst support, thus maintaining the particle size of the catalyst. Liu, Ai and Lu., Study on the Polydopamine and its derivative materials confirmed that PDA-coated structures of this nature can potentially improve the overall stability, because PDA forms a protective barrier [94].

4.2. ELECTROCHEMICAL CHARACTERIZATION

This section presents results of electrochemical characterization for the synthesized PDA/GKB40 at various coating time with respect to its activity and durability towards the Oxygen Reduction Reaction (ORR). The activity and durability of the supported catalyst is compared to commercial catalyst GKB40.

4.2.1. Cyclic Voltammetry

Cyclic voltammetry was used to electrochemically determine the electrochemical surface area (ECSA) and ORR activity of the catalyst and to determine their electrochemical durability.

Cyclic voltammograms (CV) for the synthesized PDA/GKB40 at various coating time and commercial GKB40 is shown in Figure 12. The cyclic voltammograms presented in Figure 12 shows well defined peaks. The Pt-hydride desorption peak potential appears from 0.05-0.35 V for all catalysts, the double layer region is between 0.4 and 0.7 V, the Pt-oxide formation appears around 0.7-1.2 V. The peak between 0.35 and 0.05 V is attributed to hydrogen adsorption onto the Pt surface. Figure 12 compares the voltammograms of the commercial GKB40, PDA1/GKB40 and PDA24/GKB40 in 0.1 M HClO₄. The typical voltammetric curve of Pt was observed and the ECSA of GKB40, PDA1/GKB40 and PDA24/GKB40 catalysts was determined. The ECSA was calculated from the density of charge associated to the reduction of a full monolayer of Pt oxides. This area was then converted into the effective active surface area by using the factor 210 μC.cm⁻² for the monolayer of Pt catalyst [107]. The ECSAs are presented in Table 5

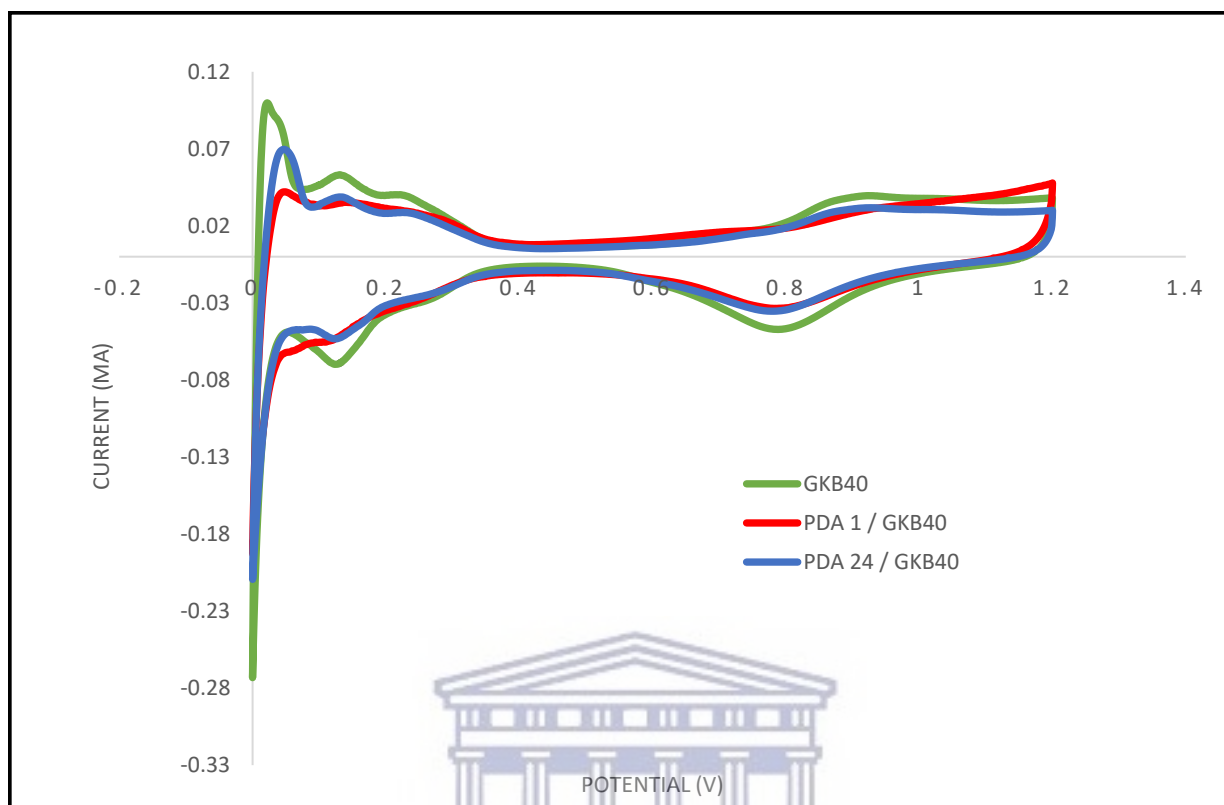


Figure 12: Cyclic voltammograms of the synthesized electrocatalyst of PDA supported on GKB40 compared to GKB40 commercial electrocatalyst in 0.1M HClO₄ at 20mV/s.

Table 5: Electrochemical surface area of GKB40 and PDA coated catalysts.

Catalyst	Pt loading (%)	ECSA (m ² Pt/g _{Pt})
GKB40	41.0%	78.6
PDA1/GKB40	43.9%	61.4
PDA24/GKB40	44.0%	59.9

The ECSA ($\text{m}^2_{\text{Pt}}/\text{g}_{\text{Pt}}$) provided in Table 5 shows that after PDA coating and calcination, the ECSA of GKB40 is decreased. This is likely due to the slight particle observed in TEM, or coating of the Pt with PDA film. This trend was observed by Taylor, S et al., they reported on a system with increasing Pt loading on carbon and observed the trend of decreasing ECSA with high loading [107]. These authors also observed similar particle sizes for all catalysts prepared, this indicated that even when agglomerated, the particles maintain the behaviour of a single particle, this was shown by the cyclic voltammetry where no changes in voltametric profile observed and the same observations were observed for this study.

4.2.2. ORR study of platinum based electro-catalysts

The ORR activity experiments were performed using Linear Sweep voltammetry (LSV) and a rotating disk electrode (RDE) (0.1M HClO_4 solution saturated with pure oxygen, 30 min). Figure 13 compares the cathodic sweeps of ORR polarization curves of the catalysts recorded at a rotational speed of 1600 rpm. The ORR curves appear in the diffusion-control region until 0.5 V then move to the mixed kinetic-diffusion control region from to 0.5 – 1.0 V, then further forward to the kinetic control region [108]. In the diffusion-controlled region, the value of ORR current density for the catalyst increased with increasing rotation speed. ORR electrocatalytic performance in this study is reported in terms of their mass-specific activities, area-specific activities and Tafel slopes at 1600 rpm at the rate of the half reaction of the system at approximately 0.9 V. The results are provided in Table 6.

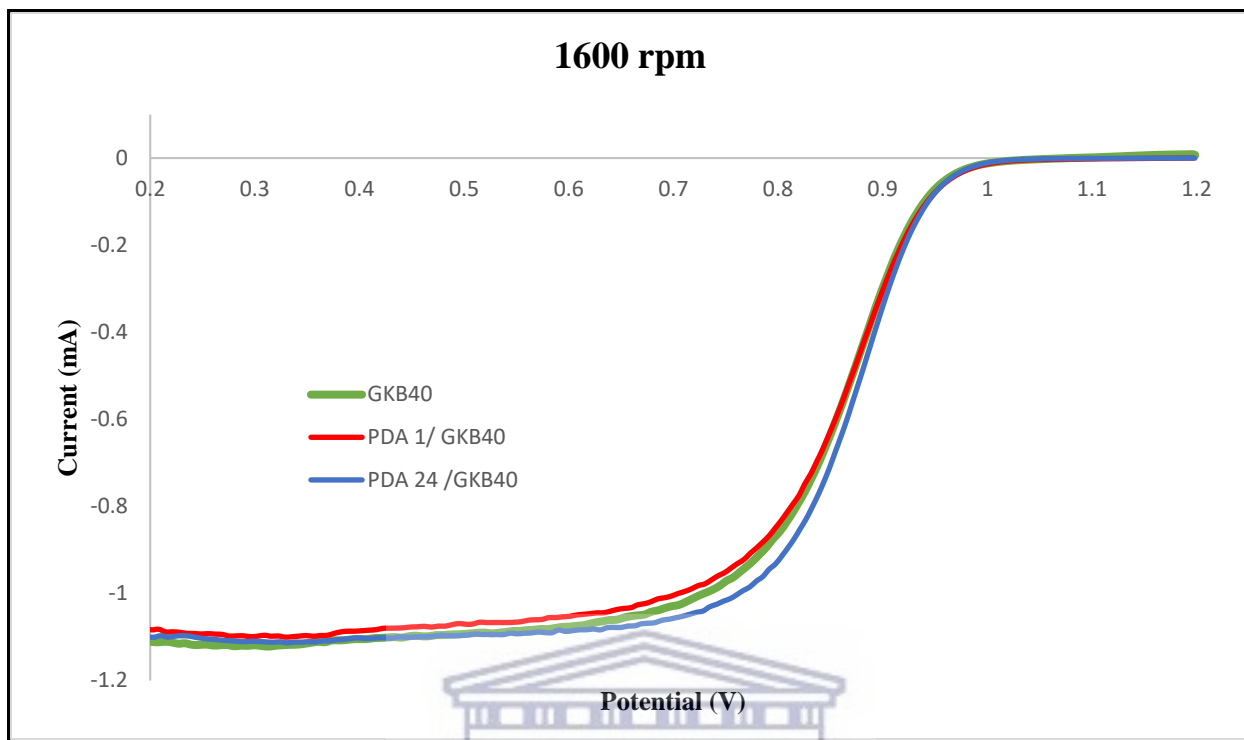


Figure 13: Polarization curves comparison of the ORR performed on GKB40 Commercial , PDA1/GKB40 and PDA24/GKB40 electrocatalysts in O₂ saturated 0.1M HClO₄ at a sweep rate of 20mV/s, rotated at 1600rpm, at room temperature.

Figure 14 provides the Tafel plots of the GKB40 commercial catalyst, PDA1/GKB40, and PDA24/GKB40 electro-catalysts obtained at 1600rpm. The plot gives a clear analysis of the ORR activity of the catalysts. From the plot it can be deduced that the activity of the catalysts is similar with PDA coated electrocatalysts having slightly lower slopes, which are provided in Table 6. The Tafel slope shows how efficiently an electrode can produce current in response to the change in applied potential. When the slope (mV/decade) is lower means less overpotential is required to get high current [109].

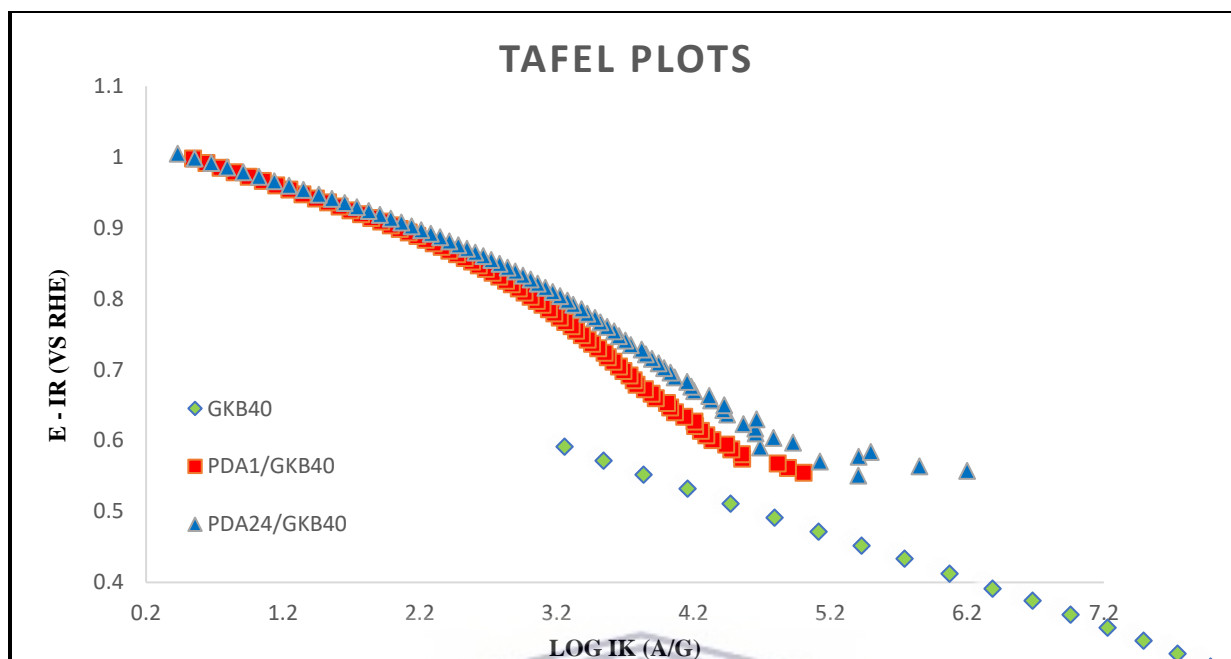


Figure 14: Mass transfer Tafel plots for the ORR on GKB40 Commercial and PDA1/GKB40, PDA25/GKB40 electro-catalysts in O₂ saturated 0.5M H₂SO₄ at a sweep rate of 20mV/s, rotating velocity of 1600rpm, at room temperature.

Table 6: The Mass specific, Area-specific and Tafel slope activities current at half reaction ($i=0.9V$) of LSV curve of GKB40, PDA1/GKB40 and PDA24/GKB40 at 1600rpm.

Electrocatalyst	Mass Specific Activity (MA) in O ₂ saturated/ (A/gPt)	Area-specific Activities (SA) in O ₂ saturated/ ($\mu A \cdot cm^{-2}$)	Slope (mV/dec)
GKB40	83.5	104.9	112.0
PDA1/GKB40	114.3	186.1	110.0
PDA24/GKB40	137.9	230.5	96.0

From Table 6, the PDA coated GKB40 electrocatalysts had higher ORR activities compared to the commercial catalyst. PDA 24hrs on GKB40 showed the largest mass and area specific activities and a lower overpotential (lower Tafel slope). Parnell et al., study on PDA coated materials, explained the dramatic shift observed in the ORR potential possibly lies within the interaction between PDA and carbon contained support material. The nitrogen atoms in PDA interacts with the sp^2 carbon network in GKB, which creates defects in the adjacent sites. This, in turn, changes in the charge density, resistance in charge transfer, and hydrophilicity of the material to assist in ORR. Moreover, the charge density change can affect the contact of the dissolved oxygen molecules on the PDA coated electrocatalysts. The oxygen bond is weakened, allowing for easier ORR. Thus, when PDA interacts with GKB, the conjugated system is delocalized between the sp^2 carbon framework in GKB and the lone pairs of electrons on the nitrogen in PDA to give better electrochemical transfer towards ORR with a lower overpotential [110].

4.2.3 Electrochemical durability of GKB40 electrocatalysts

To determine the electrochemical durability of the catalyst, an accelerated degradation testing (ADT) was conducted in 0.1M HClO₄. The catalyst layer is exposed to the electrolyte solution to mimic the environment of electrode membrane interface in PEMFC. The synthesized catalysts were tested to assess the corrosion resistance in similar conditions to those employed in a PEMFC, following the procedure described in Section 3.2.2.2. The loss of Pt was evaluated periodically during the carbon degradation test, by monitoring the ECSA loss. The comparison of electrochemical behaviours of the catalysts supported on GKB before and after potential cycling are presented in Figure 15. The catalysts supported on GKB demonstrated changes in the hydrogen adsorption peaks during potential cycling.

The current intensity of the voltammograms of GKB40, PDA1/GKB40 and PDA24/GKB40 catalysts obtained after potential cycling dropped with potential cycling, indicating a degradation in electrocatalytic activity. The percentage ECSA loss with cycling number up to 5000 cycles is plotted in Figure 16 and the results are provided in Table 7.

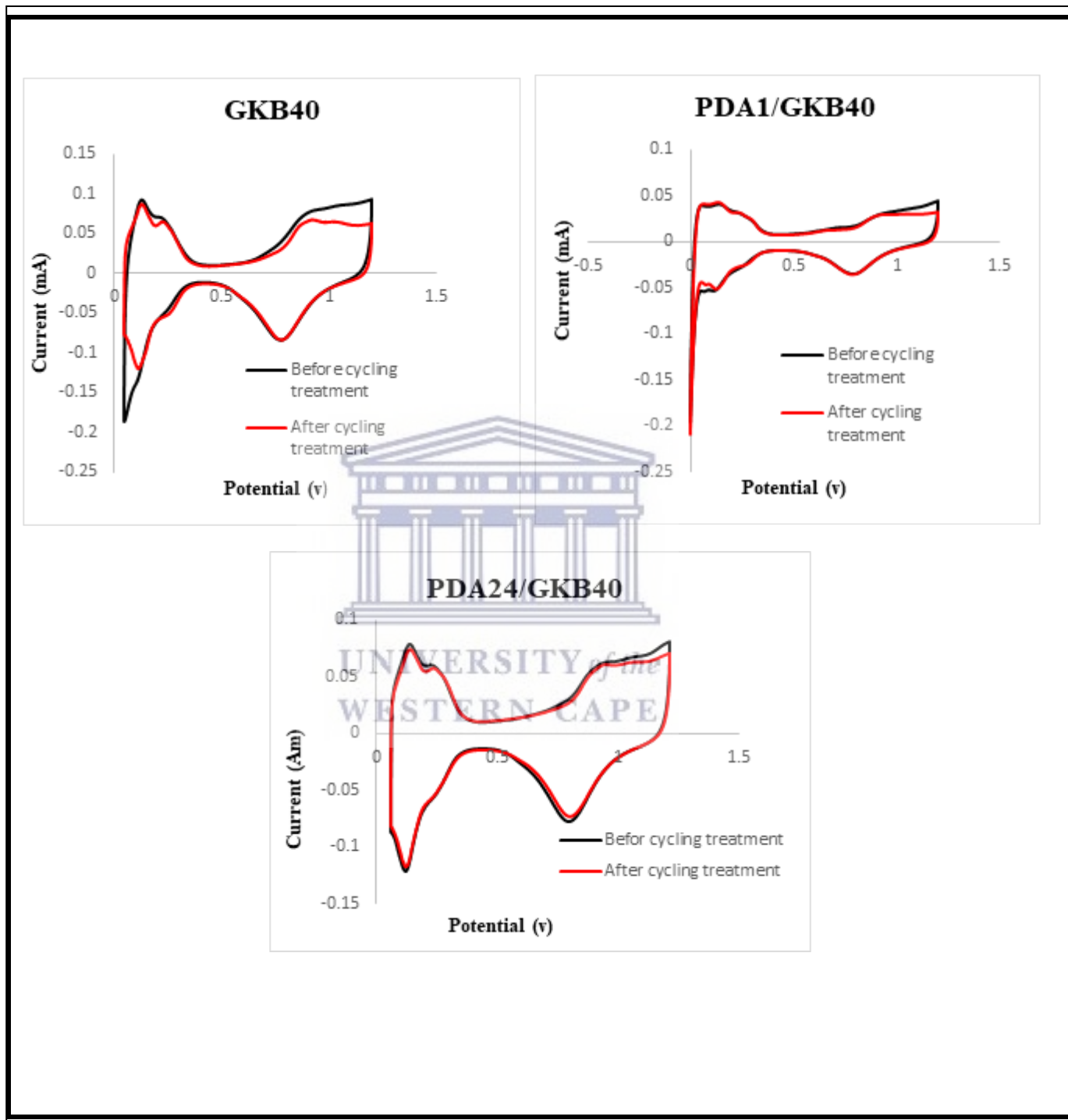


Figure 15: Cyclic voltammograms of GKB40, PDA1/GKB40 and PDA24/GKB40 catalysts before and after the cycling

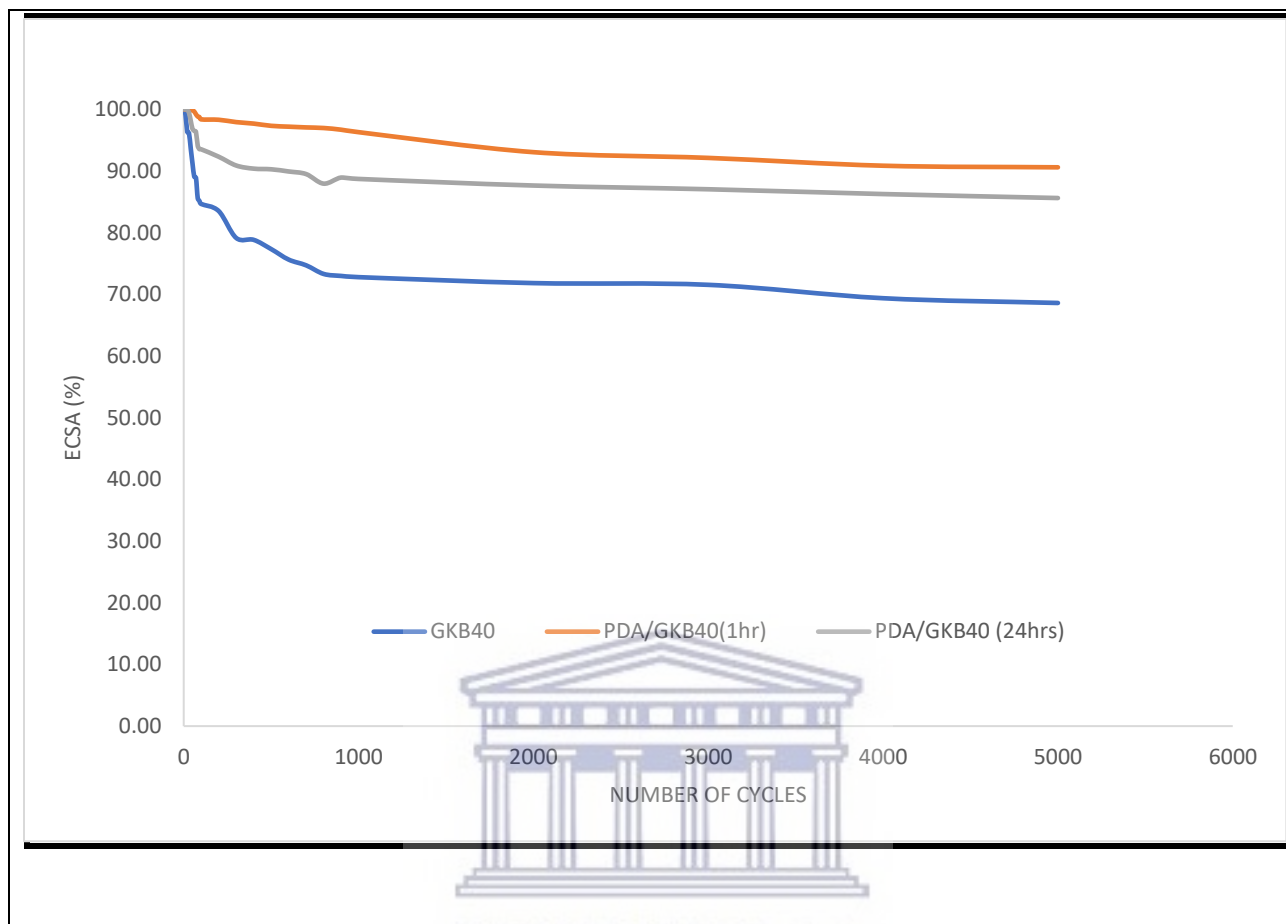


Figure 16: The ECSA% determined after every 100 cycles until 5000 cycles for commercial GKB40, PDA1/GKB40 and PDA24/GKB40 in 0.1 M HClO₄.

Table 7: The ECSA loss determined after 5000 cycles of GKB40, PDA1/GKB40 and PDA24/GKB40

Electrocatalysts	Loss in ECSA (%)
GKB40	31.4
PDA1/GKB40	9.4
PDA24/GKB40	14.4

The loss in Pt ECSA because of carbon corrosion is evidenced by the decrease in hydrogen adsorption/desorption peaks shown between 0.05-0.35 V potential region, the most visible change was observed for uncoated GKB40 (Table 7). The major rate of degradation was observed for the first 100 cycles for both coated and uncoated catalysts followed by the second rate up until 1000 cycles for GKB40 catalyst only and then remained constant till 5000 cycles were reached. The ECSA of commercial GKB40 decreased significantly faster than PDA coated having a total loss of 31.4% after 5000 cycles compared to only 9.1 % for PDA1/GKB40 and 14.4% for PDA24/GKB40 electrocatalysts. Electrochemical carbon corrosion decreased the amount of carbon available for Pt loading, which forced the Pt nanoparticles to migrate on the carbon surface and aggregate at relatively stable sites, explained by the study of Jang and Kim Study on the effect of water electrolysis catalysts on carbon corrosion in PEMFCs [111]. The PDA coated catalysts displayed higher stability and resistance to corrosion compared to commercial GKB40, verifying that carbon support have improved corrosion resistance in acidic media in the presence of PDA films that acted as a protective barrier against harsh oxidative environment.

Stability studies of PDA-coated nanocomposite also showed catalytic activity in a wide pH range which is advantageous in fuel cell application [110]. When this nanocomposite was coated with PDA, the multicomponent material revealed a significant increase in ORR performance. Varying the pH revealed increased current density in alkaline media accompanied with slightly high overpotential. Literature study by Parnell et al., also stated that during the formation of the PDA coating, the Mn (III) complex was reduced to a Mn (II) complex. This oxidation state changed, along with the possible interaction of PDA with graphene, furnished a nanocomposite with enhanced ORR activity. Furthermore, the RRDE ring current did not increase, which suggests that no hydroperoxide intermediate is involved in the ORR mechanism. To their knowledge this was the first use of a PDA-MN-graphene nanocomposite for ORR applications [110].

CHAPTER FIVE

CONCLUSIONS AND RECOMMENDATIONS

The aim of this work was to increase the durability of a carbon supported Pt catalyst without compromising its performance toward the ORR. To this end, a commercial catalyst, GKB40 was coated with polydopamine (PDA), the final oxidation product of dopamine.

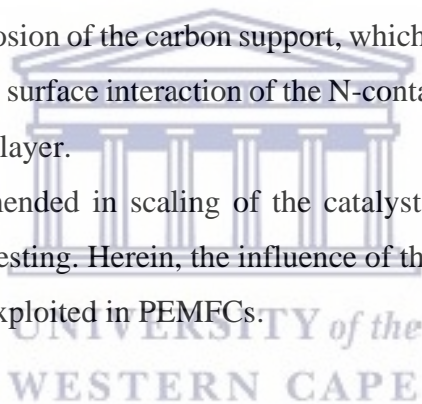
The PDA/GKB40 catalyst was successfully synthesized. The synthesized PDA/GKB and PDA/GKB40 electro-catalysts were deposited at two different deposition times (1h and 24hrs) whereafter they were calcined at 400°C in N₂. These catalysts then underwent physical characterization using FTIR, TGA and HRTEM. FTIR analysis of PDA coated catalysts confirmed a more complex material as compared to uncoated catalyst by the presence of absorbances corresponding to the functional groups in PDA. TGA was then performed on the synthesized and commercial samples to estimate the amount of PDA deposited and whether the calcination degraded the catalyst. Approximately 20% of PDA material was deposited on PDA/GKB40 catalysts for 1hr deposition time. Degradation due to carbon oxidation in GKB40 catalyst only took place at high temperatures attributed to carbon degradation from GKB material. After calcination the mass loading of Pt catalyst remaining in all the samples was determined and GKB40 commercial was observed to have approximately 3% less in Pt mass composition as compared to PDA coated GK40 catalysts. HRTEM images produced well dispersed Pt nanoparticles with majority of the particles in the size range of 3-5 nm for synthesized and commercial catalysts. There was a slight increase in the particle size after PDA deposition and calcination that could be due to agglomeration of the nanoparticles at high temperature.

An electrochemical benchmarking study was then performed to determine the activity and durability of the ORR catalyst with respect to two PDA coated GKB40 and commercial GKB40 electrocatalysts. The synthesized catalysts PDA1/GKB40 and PDA24/GKB40 catalysts had better mass specific activity of 114.3 A/g, 137.9 A/g and area specific activity of 186.1 $\mu\text{A} \cdot \text{cm}^{-2}$, 230.5 $\mu\text{A} \cdot \text{cm}^{-2}$ compared to the benchmark. The PDA coated electrocatalysts also presented with lower Tafel slopes of 110 mV/dec, compared to 112 mV/dec for GKB40.

The corrosion resistance of PDA/GKB40 coated and uncoated GKB40 electrocatalysts materials was evaluated by subjecting the catalysts to a potential cycling. 31.9% of the commercial GKB40 ECSA was lost after 5000 potential cycles and only 9.1% for PDA1/GKB40 and 14,1% for PDA24/GKB40. ECSA decay in both PDA coated and un-coated GKB40 catalysts was caused by Pt loss due to carbon support degradation. These results showed that the synthesized PDA coated catalyst maintained the ORR activity while improving the durability compared to the commercial GKB40.

In conclusion the objectives of the study were achieved. The addition of PDA thin film onto the surface of Pt catalyst improved the durability without effecting the performance of Pt catalyst in PEM fuel cells. This study therefore recommends that the PDA/GKB40 should be used over the Pt commercial catalysts in PEMFC applications. The PDA thin film slows the degradation of platinum catalyst, caused by corrosion of the carbon support, which is the major contributing factor of catalyst layer degradation. The surface interaction of the N-containing PDA, inhibit degradation and likely constitute a sacrificial layer.

Further studies are also recommended in scaling of the catalyst and including in a membrane electrode assembly for fuel cell testing. Herein, the influence of the PDA and supporting material interactions can be studied and exploited in PEMFCs.



REFERENCES

- [1] Arif, M., Cheung, S.C.P. & Andrews, J., 2019a, “A systematic approach for matching simulated and experimental polarization curves for a PEM fuel cell,” *International Journal of Hydrogen Energy*.
- [2] Hoel, M. (1996) ‘Depletion of fossil fuels and the impacts of global warming’, Science Direct. Elsevier Ltd,18 (0928), pp. 115–136.
- [3] Herzog, A. V., Lipman, T. E. and Kammen, D. M. (2001) ‘Renewable energy sources’, *Environment*, Vol. 43 No. 10. pp. 1–63.
- [4] Of, N. T. and Of, A. T. E. S. (2001) ‘Renewable Energy; An Overview’: U.S. Department of Energy (DOE). *Energy Efficiency and Renewable Energy*. pp.1-8
- [5] World’s first hydrogen-powered zero-emission combustion engine launched. (2018, April 23). Governemnt europa. Retrieved from <https://www.governmenteuropa.eu>
- [6] Elmer, T., Worall, M., Wu, S. and Riffat, S.B., 2015. Fuel cell technology for domestic built environment applications: State of-the-art review. *Renewable and Sustainable Energy Reviews*, 42, pp.913-931.
- [7] Stacy, J., Regmi, Y. N., Leonard, B. and Fan, M., 2017. The recent progress and future of oxygen reduction reaction catalysis: A review. *Renewable and Sustainable Energy Reviews*, 69, pp.401-414.
- [8] Castanheira, L. et al. (2015) ‘Carbon Corrosion in Proton-Exchange Membrane Fuel Cells: Effect of the Carbon Structure, the Degradation Protocol, and the Gas Atmosphere’, *ACS Catalysis*, 5(4), pp. 2184–2194.

- [9] Jourdan, M., Mounir, H., & El Marjani, A. (2014). Compilation of factors affecting durability of Proton Exchange Membrane Fuel Cell (PEMFC). (pp. 542-547). Ouarzazate: 2014 *International Renewable and Sustainable Energy Conference (IRSEC)*. doi:10.1109/IRSEC.2014.7059906
- [10] Thiam, H. S., Daud, W.R.W., Kamarudin, S. K., Mohammad, A. B., Kadhum, A.A.H., Loh, K.S. & Majlan, E.H., 2011, *Overview on nanostructured membrane in fuel cell applications, International Journal of Hydrogen Energy*, 36(4), 3187–3205.
- [11] Werner, C., Gores, F., Busemeyer, L., Kallo, J., Heitmann, S. & Griebenow, M., no date, characteristics of pemfc operation in ambient and low-pressure environment considering the fuel cell humidification.
- [12] Liu, Y., Ai, K. & Lu, L. Polydopamine and its derivative materials: *synthesis and promising applications in energy, environmental, and biomedical fields. Chem. Rev.* 114, 5057–5115 (2014).
- [13] Sharaf, O. Z. and Orhan, M. F., 2014. An overview of fuel cell technology: *Fundamentals and applications. Renewable and Sustainable Energy Reviews*, 32, pp.810-853.
- [14] Fernandez Alvarez, G., 2011. *Palladium based catalysts for oxygen reduction in polymer electrolyte membrane fuel cells* (Doctoral thesis, Newcastle University). [accessed online, 28 February 2017].
- [15] R. S. Khurmi and R. S. Sedha, *Material Science, Ed. 4*, ISBN 8121901464. (2008): p. 18
- [16] Thangavelautham, J., 2018, “Degradation in PEM Fuel Cells and Mitigation Strategies Using System Design and Control,” *Proton Exchange Membrane Fuel Cell, InTech*.
- [17] Ralph, T. R. & Hogarth, M. P., no date, *Catalysis for Low Temperature Fuel Cells PART I: The cathode challenges*.

- [18] Spiegel, D. C. (2017, 01 23). History of Fuel Cell. Retrieved from *Fuel Cell Store*: <https://www.fuelcellstore.com/blog-section/history-of-fuel-cells>.
- [19] Lysik, A., Wejrzanowski, T., Cwieka, K., Skibinski, J., Milewski, J., Marques, F.M.B., Norby, T. & Xing, W., 2020, “Silver coated cathode for molten carbonate fuel cells,” *International Journal of Hydrogen Energy*, 45(38), 19847–19857.
- [20] Sundmacher, K., Schultz, T., Zhou, S., Scott, K., Ginkel, M. & Gilles, E.D., no date, Dynamics of the direct methanol fuel cell (DMFC): *experiments and model-based analysis*.
- [21] Moallemi, E. A., Ahmadi, A., Afraze, A. & Moghaddam, N.B., 2015, “Assessing the Performance of Transition Towards Renewable Energy: Case Study of Iran’s Fuel Cell Technology,” *Journal of Corporate Citizenship*, 2015(58), 137–158.
- [22] Choudhury, Suman Roy, Choudhury, Suhasini Roy, Rangarajan, J. & Rengaswamy, R., 2005, “Step response analysis of phosphoric acid fuel cell (PAFC) cathode through a transient model,” *Journal of Power Sources*, 140(2), 274–279.
- [23] Kargupta, K., Saha, S., Banerjee, D., Seal, M. & Ganguly, S., 2012, “Performance enhancement of phosphoric acid fuel cell using phosphosilicate gel-based electrolyte,” *RanliaoHuaxueXuebao/Journal of Fuel Chemistry and Technology*, 40(6), 707–713.
- [24] Rai, V., 2008, Molecular modeling of PEM fuel cell electrochemistry.
- [25] Chalk, S. G. & Miller, J. K., 2006, “Key challenges and recent progress in batteries, fuel cells, and hydrogen storage for clean energy systems,” *Journal of Power Sources*, 159(1 SPEC. ISS.), 73–80.
- [26] Wee, J. H. (2007) ‘Applications of proton exchange membrane fuel cell systems’, *Renewable and Sustainable Energy Reviews*, 11(8), pp. 1720–1738. doi: 10.1016/j.rser.2006.01.005

- [27] Vaghari, H. et al. (2013) ‘Recent advances in application of chitosan in fuel cells’, *Sustainable Chemical Processes*, 1(1), p. 16. doi: 10.1186/2043-7129-1-16.
- [28] Esfeh, H. K. & Hamid, M. K. A., 2014, Temperature effect on proton exchange membrane fuel cell performance Part II: *Parametric study*, *Energy Procedia*, vol. 61, 2617–2620, Elsevier Ltd.
- [29] Shah, R. K., “Introduction to fuel cells,” *Recent Trends Fuel Cell Sci. Technol.*, no. 1, pp. 1–9, 2007.
- [30] Suurs, R. A. A., Hekkert, M. P. & Smits, R.E.H.M., 2009, “Understanding the build-up of a technological innovation system around hydrogen and fuel cell technologies,” *International Journal of Hydrogen Energy*, 34(24), 9639–9654.
- [31] Thangavelautham, J., 2018, “Degradation in PEM Fuel Cells and Mitigation Strategies Using System Design and Control,” *Proton Exchange Membrane Fuel Cell, InTech*.
- [32] Grove, W. R., On a gaseous voltaic battery, *Philosophical magazine and journal of science*. 101, (1842): p.417-420
- [32] Thiam, H. S., Daud, W. R.W., Kamarudin, S. K., Mohammad, A. B., Kadhum, A. A. H., Loh, K. S. & Majlan, E. H., 2011, Overview on nanostructured membrane in fuel cell applications, *International Journal of Hydrogen Energy*, 36(4), 3187–3205.
- [33] Pauchet, J., Prat, M., Schott, P., Kuttanikkad, S. P. & Pulloor, S., 2012, “Performance loss of proton exchange membrane fuel cell due to hydrophobicity loss in gas diffusion layer: Analysis by multiscale approach combining pore network and performance modelling,” *International Journal of Hydrogen Energy*, 37, 1628–1641.
- [34] Hartnig, C., Jörisen, Kerres, J., Lehnert, W., and Scholta, J., Polymer electrolyte membrane fuel cells. *Woodhead Publishing Limited*, 2008

- [35] “Form in Place/ Cure in Place Gaskets.” [Online]. Available: <https://www.dymax.com/index.php/en/adhesives/fip-gaskets>. [Accessed: 12Aug-2015].
- [36] Page, P. M., “Sealing sense,” *Pumps*, no. September, pp. 46–47, 2004.
- [37] Shah, R. K., “Introduction to fuel cells,” *Recent Trends Fuel Cell Sci. Technol.*, no. 1, pp. 1–9, 2007.
- [38] Ohenoja, M., Sorsa, A. & Leiviskä, K., 2018, *Model structure optimization for fuel cell polarization curves*, *Computers*, 7(4).
- [39] Sundmacher, K., Schultz, T., Zhou, S., Scott, K., Ginkel, M. & Gilles, E.D., no date, *Dynamics of the direct methanol fuel cell (DMFC): experiments and model-based analysis*.
- [40] Anslyn, E. V., and Dougherty, D. A., *Modern Physical organic chemistry*. 490, (2006).
- [41] Appleby, A., and Foulkes, F., *Fuel cell handbook*, Van Nostrand Reinhold, New York, USA. (1989): p.762.
- [42] Mayrhofer, K. J. J., et al., Measurement of oxygen reduction activities via the rotating disc electrode method: From Pt model surfaces to carbon-supported high surface area catalysts. *Electrochimica Acta*, 2008. 53(7): p. 3181-3188.
- [43] Fernandez Alvarez, G., 2011. Palladium based catalysts for oxygen reduction in polymer electrolyte membrane fuel cells (Doctoral thesis, Newcastle University). [accessed online, 28 February 2017].
- [44] Calderón, J. C., Ndzuzo, L., Bladergroen, B. J. and Pasupathi, S., 2018. Catalytic activity of carbon supported-Pt-Pd nanoparticles toward the oxygen reduction reaction. *Materials Today: Proceedings*, 5(4), pp.10551-10560.
- [45] Sharma, S. and Pollet, B. G., 2012. Support materials for PEMFC and DMFC electrocatalysts—a review. *Journal of Power Sources*, 208, pp.96-119.

- [46] Jha, N., Reddy, A. L. M., Shaijumon, M. M., Rajalakshmi, N. and Ramaprabhu, S., 2008. Pt–Ru/multi-walled carbon nanotubes as electrocatalysts for direct methanol fuel cell. *International Journal of Hydrogen Energy*, 33(1), pp.427-433.
- [47] Yu, X. and Ye, S., 2007. Recent advances in activity and durability enhancement of Pt/C catalytic cathode in PEMFC: Part I. Physico-chemical and electronic interaction between Pt and carbon support, and activity enhancement of Pt/C catalyst. *Journal of Power Sources*, 172(1), pp.133-144.
- [48] Stacy, J., Regmi, Y. N., Leonard, B. and Fan, M., 2017. The recent progress and future of oxygen reduction reaction catalysis: A review. *Renewable and Sustainable Energy Reviews*, 69, pp.401-414.
- [49] Wang, J., Yin, G., Shao, Y., Zhang, S., Wang, Z. and Gao, Y., 2007. Effect of carbon black support corrosion on the durability of Pt/C catalyst. *Journal of Power sources*, 171(2), pp.331-339.
- [50] Wang, Y., Jin, J., Yang, S., Li, G. and Qiao, J., 2015. Highly active and stable platinum catalyst supported on porous carbon nanofibers for improved performance of PEMFC. *Electrochimica Acta*, 177, pp.181-189.
- [51] Wang, X., Li, W., Chen, Z., Waje, M. and Yan, Y., 2006. Durability investigation of carbon nanotube as catalyst support for proton exchange membrane fuel cell. *Journal of Power Sources*, 158(1), pp.154-159.
- [52] Figueiredo, J. L. and Pereira, M. F., 2013. Synthesis and functionalization of carbon xerogels to be used as supports for fuel cell catalysts. *Journal of Energy Chemistry*, 22(2), pp.195-201.

- [53] Stambula, S., Gauquelin, N., Bugnet, M., Gorantla, S., Turner, S., Sun, S., Liu, J., Zhang, G., Sun, X. and Botton, G.A., 2014. Chemical structure of nitrogen-doped graphene with single platinum atoms and atomic clusters as a platform for the PEMFC electrode. *The Journal of Physical Chemistry C*, 118(8), pp.3890-3900.
- [54] Antolini, E., 2009. Carbon supports for low-temperature fuel cell catalysts. *Applied Catalysis B: Environmental*, 88(1-2), pp.1-24.
- [55] Dickinson, A. J., Carrette, L. P. L., Collins, J. A., Friedrich, K. A. and U. Stimming, *Electrochim.Acta*. 47, (2002): p.3733.
- [56] McLean, G. F., et al., An assessment of alkaline fuel cell technology. *International Journal of Hydrogen Energy*, 2002. 27(5): p. 507-526.
- [57] Strasser, P., et al., Lattice-strain control of the activity in dealloyed core-shell fuel cell catalysts. *Nature Chemistry*, 2010. 2(6): p. 454-460.
- [58] Wang, C., Markovic, N. M., and Stamenkovic, V. R., Advanced Platinum Alloy Electrocatalysts for the Oxygen Reduction Reaction. *Acs Catalysis*, 2012. 2(5): p. 891-898.
- [59] Min, M., Cho, J. Cho, K. Kim, H., Particle size and alloying effects of Pt-based alloy electro-catalysts for fuel cell applications, *Electrochimica Acta*. 45, (2000): p.4211– 4217.
- [60] Mansor, N., 2013. Development of Catalysts and Catalyst Supports for Polymer Electrolyte Fuel Cells. Ph.D. University College London.
- [61] He, C., Desai, S. Brown, G. and Bollepalli, S. PEM fuel cell electro-catalysts: Cost, performance, and durability, *The electrochemical society Interface*. (2005): p.41-44.
- [62] Shao, Y. Y., Liu, J., Wang, Y., Lin, Y. H., Novel catalyst support materials for PEM fuel cells: Current status and future prospects, *J. Mater Chem*. 19, (2009): p.46-59.

- [63] Gong, Y. Synthesis, characterization and performance of Pt-based electro-catalysts for low temperature fuel cells, (2008): p.17-20.
- [64] Wang, S., Nanostructured electro-catalysts for proton exchange membrane fuel cells (PEMFC), Phd thesis, Nanyang Technological University, Singapore. (2010).
- [65] Oh, H. S. et al. (2016) 'Electrochemical Catalyst-Support Effects and Their Stabilizing Role for IrO_x Nanoparticle Catalysts during the Oxygen Evolution Reaction', *Journal of the American Chemical Society*, 138(38), pp. 12552–12563. doi: 10.1021/jacs.6b07199.
- [66] Antolini, E. and Gonzalez, E. R. (2009) 'Ceramic materials as supports for low-temperature fuel cell catalysts', *Solid State Ionics*. Elsevier B.V., 180(9–10), pp. 746–763. doi: 10.1016/j.ssi.2009.03.007.
- [67] Sadhasivam, T. et al. (2016) 'Graphitized carbon as an efficient mesoporous layer for unitized regenerative fuel cells', *International Journal of Hydrogen Energy*. Elsevier Ltd, 41(40), pp. 18226–18230. doi: 10.1016/j.ijhydene.2016.08.092.
- [68] Castanheira, L. et al. (2015) 'Carbon Corrosion in Proton-Exchange Membrane Fuel Cells: Effect of the Carbon Structure, the Degradation Protocol, and the Gas Atmosphere', *ACS Catalysis*, 5(4), pp. 2184–2194.
- [69] Travassos, M. A. and Rangel, C. M. (2010) 'Polarity Reversal in PEM Fuel Cells by Fuel Starvation', pp. 48–52.
- [70] Zhang, S. et al. (2000) 'A phenomenological approach for the Id/Ig ratio and sp³ fraction of magnetron sputtered a-C films', *Surface and Coatings Technology*, 123(2–3), pp. 256–260. doi: 10.1016/S0257-8972(99)00523-X.
- [71] Wilkinson, D. P. and St-Pierre, J. (2003) 'Durability', in *Handbook of fuel Cells - Fundamentals, Technology and Applications*, pp. 611–626.

- [72] Perry, M. L., Patterson, T. and Reiser, C. (2006) 'Systems Strategies to Mitigate Carbon Corrosion in Fuel Cells', *ECS Transactions*, 3(September), pp. 783–795. doi: 10.1149/1.2356198.
- [73] Yu, Y. et al. (2012) 'A review on performance degradation of proton exchange membrane fuel cells during startup and shutdown processes: Causes, consequences, and mitigation strategies', *Journal of Power Sources*, 205, pp. 10–23. doi: 10.1016/j.jpowsour.2012.01.059.
- [74] He, C., Desai, S., Brown, G. and Bollepli, S., 2005. PEM Fuel Cell Catalysts: Cost, Performance, and Durability. *The Electrochemical Society Interface*, 14(3), pp.41-44.
- [75] Cleghorn, S., Mayfield, D., Moore, D., Moore, J., Rusch, G., Sherman, T., . . . Beuscher, U. (2006). A polymer electrolyte fuel cell life test: 3 years of continuous operation. *Journal of Power Sources*, 158, 54- 446.
- [76] Jouin, M., Gouriveau, R., Hissel, D., Péra, M.-C., & Zerhouni, N. (2013). Prognostics and Health Management of PEMFC – State of the art and remaining challenges. *International Journal of Hydrogen Energy*, 38(35), 15307-15317.
- [77] Wang, H. H., Li, H., and Yuan, X.-Z., "Introduction," in PEM Fuel Cell Failure Mode, Wang Haijiang Henry; Li Hui; Yuan Xiao-Zi, Ed. Boca Raton, Fla.: CRC, 2012, pp. 1–2.
- [78] Dhathathreyan K.S; Rajalakshmi N., "Polymer Electrolyte Membrane Fuel Cell," in Title: Recent Trends Fuel Cell Science and Technology, S. Basu, Ed. Springer and Anayama, 2007, pp 40-115.
- [79] Eriksson, M., Lindbergh, G., Eriksson, B. & Jansson, A., no date, Accelerated degradation of bipolar plates in the PEMFC Accelereradnedbryningavbipoläraplattori en PEMFC.
- [80] Energy R. and Energy, A. (1950) 'Renewable energy and other alternative energy sources', Energy. Chapter 12. pp. 149–157.

- [81] Yu, P. T.; Gu, W.; Zhang, J.; Makharia, R.; Wagner, F. T.; Gasteiger, H. A., Carbon-Support Requirements for Highly Durable Fuel Cell Operation. In *Polymer Electrolyte Fuel Cell Durability*, Buchi, F. N.; Inaba, M.; Schmidt, T. J., Eds. Springer: 2009; pp 41-42.
- [82] H. A. Gasteiger, Keynote Lecture presented at 19th North American Catalysis Society Meeting, Philadelphia, PA (2005).
- [83] Oh, H.-S., J.-G. Oh, and Kim, H., Modification of polyol process for synthesis of highly platinum loaded platinum-carbon catalysts for fuel cells. *J. Power Sources*, 2008. 183(2):p. 600-603.
- [84] Kinoshita, K., *Carbon Electrochemical and Physicochemical Properties*, J. Wiley & Sons, New York, NY (1988).
- [85] Roen, L., Paik, C., and Jarvi, T. "Electrocatalytic corrosion of carbon support in PEMFC cathodes," *Electrochemical and Solid-State Letters*, Vol. 7, No. 1, pp. A19-A22 (2004).
- [86] Yu, X. and Ye, S., 2007. Recent advances in activity and durability enhancement of Pt/C catalytic cathode in PEMFC. *Journal of Power Sources*, 172(1), pp.133-144.
- [87] Li, W. and Lane, A., 2009. Investigation of Pt catalytic effects on carbon support corrosion of the cathode catalyst in PEM fuel cells using DEMS spectra. *Electrochemistry Communications*, 11(6), pp.1187-1190.
- [88] Yu, Y. et al. (2012) 'A review on performance degradation of proton exchange membrane fuel cells during startup and shutdown processes: Causes, consequences, and mitigation strategies', *Journal of Power Sources*, 205, pp. 10–23. doi: 10.1016/j.jpowsour.2012.01.059.
- [89] Zhao, L., Zhu, J., Zheng, Y., Xiao, M., Gao, R., Zhang, Z., Wen, G., Dou, H., Deng, Y., Yu, A., Wang, Z. and Chen, Z., 2021. Materials Engineering toward Durable Electrocatalysts for Proton Exchange Membrane Fuel Cells. *Advanced Energy Materials*, p.2102665.

- [90] Qiao, Z., Hwang, S., Li, X., Wang, C., Samarakoon, W., Karakalos, S., Li, D., Chen, M., He, Y., Wang, M., Liu, Z., Wang, G., Zhou, H., Feng, Z., Su, D., Spendelow, J. and Wu, G., 2019. 3D porous graphitic nanocarbon for enhancing the performance and durability of Pt catalysts: a balance between graphitization and hierarchical porosity. *Energy & Environmental Science*, 12(9), pp.2830-2841.
- [91] Che, D., Cheng, J., Ji, Z., Zhang, S., Li, G., Sun, Z. & You, J., 2017, Recent advances and applications of polydopamine-derived adsorbents for sample pretreatment, *TrAC - Trends in Analytical Chemistry*, 97, 1–14.
- [92] Lin, M., Huang, H., Liu, Y., Liang, C., Fei, S., Chen, X. & Ni, C., 2013, “High loading of uniformly dispersed Pt nanoparticles on polydopamine coated carbon nanotubes and its application in simultaneous determination of dopamine and uric acid,” *Nanotechnology*, 24(6).
- [93] Chung, D. Y. et al. Highly durable and active PtFe nanocatalyst for electrochemical oxygen reduction reaction. *J. Am. Chem. Soc.* 137, 15478–15485 (2015).
- [94] Liu, Y., Ai, K. & Lu, L. Polydopamine and its derivative materials: synthesis and promising applications in energy, environmental, and biomedical fields. *Chem. Rev.* 114, 5057–5115 (2014).
- [95] Dhathathreyan K. S; Rajalakshmi N., “Polymer Electrolyte Membrane Fuel Cell,” in Title: Recent Trends Fuel Cell Science and Technology, S. Basu, Ed. Springer and Anayama, 2007, pp 40-115.
- [96] Werner, C., Gores, F., Busemeyer, L., Kallo, J., Heitmann, S. & Griebenow, M., no date, characteristics of pemfc operation in ambient and low-pressure environment considering the fuel cell humidification.
- [97] Monk, P. (2001). *Fundamentals of Electro-Analytical Chemistry*. Singapore: Wiley & Sons.

- [98] Wu, J., Yuan, X., Wang, H., Blanco, M., Martin, J., & Zhang, J. (2008). Diagnostic tools in PEM fuel cell research: Part I Electrochemical techniques. *International Journal of Hydrogen Energy*, 33(6), 1735-1746.
- [99] Calculation of the platinum's active surface. (2005). Retrieved from Bio-logic Science Instruments: www.bio-logic.net.
- [100] Li, W. and Lane, A., 2009. Investigation of Pt catalytic effects on carbon support corrosion of the cathode catalyst in PEM fuel cells using DEMS spectra. *Electrochemistry Communications*, 11(6), pp.1187-1190.
- [101] S. Srinivasan, Fuel cells: Fundamentals to applications. P. 299.
- [102] Zhao, J., Tu, Z. and Chan, S., 2021. Carbon corrosion mechanism and mitigation strategies in a proton exchange membrane fuel cell (PEMFC): A review. *Journal of Power Sources*, 488, p.229434.
- [103] Garland, N., Benjamin, T., & Kopasz, J. (2007). DOE Fuel Cell Program: Durability Technical Targets and Testing Protocols. *ECS Transactions*, 11(1), 923. doi:10.1149/1.2781004.
- [104] Coskun, H., Aljabour, A., Uiberlacker, L., Strobel, M., Hild, S., Cobet, C., Farka, D., Stadler, P. and Sariciftci, N., 2018. Chemical vapor deposition - based synthesis of conductive polydopamine thin-films. *Thin Solid Films*, 645, pp.320-325.
- [105] Zhao, L., Bi, D., Qi, X., Guo, Y., Yue, F., Wang, X. and Han, M., 2019. Polydopamine-based surface modification of paclitaxel nanoparticles for osteosarcoma targeted therapy. *Nanotechnology*, 30(25), p.255101.
- [106] Damberga, D., Fedorenko, V., Grundšteins, K., Altundal, Ş., Šutka, A., Ramanavičius, A., Coy, E., Mrówczyński, R., Iatsunskyi, I. and Viter, R., 2020. Influence of PDA Coating on the Structural, Optical and Surface Properties of ZnO Nanostructures. *Nanomaterials*, 10(12), p.2438.

- [107] Taylor, S. et al., 2016. The effect of platinum loading and surface morphology on oxygen reduction activity. *Electrocatalysis*, 7(4), pp.287–296.
- [108] Vincent, I., 2016. Electrochemical Characterization and Oxygen Reduction Kinetics of Cu-incorporated Cobalt Oxide Catalyst. *International Journal of Electrochemical Science*, pp.8002-8015.
- [109] Tryk, D., Lee, M., Uchida, M., Uchida, H. and Watanabe, M., 2019. Tafel Slope Component Analysis of Polymer Electrolyte Fuel Cell Cathode Current-Potential Behavior. *ECS Transactions*, 35(27), pp.13-23.
- [110] Parnell, C., Chhetri, B., Brandt, A., Watanabe, F., Nima, Z., Mudalige, T., Biris, A. and Ghosh, A., 2016. Polydopamine-Coated Manganese Complex/Graphene Nanocomposite for Enhanced Electrocatalytic Activity Towards Oxygen Reduction. *Scientific Reports*, 6(1).
- [111] Jang, S. and Kim, H., 2010. Effect of Water Electrolysis Catalysts on Carbon Corrosion in Polymer Electrolyte Membrane Fuel Cells. *Journal of the American Chemical Society*, 132(42), pp.14700-14701.

